Measuring Linear Urban Land Expansion:

A Literature Review & Case Study of the City of Calgary

Phillip Burrows

Department of Geography,

University of Calgary

Under the supervision of Dr. Eliot Tretter

December 10th, 2020

Abstract

The object of this paper was to develop a methodology for determining the linear urban land expansion of the City of Calgary in recent decades. Academic literature was reviewed that described four principal drivers of urban land expansion globally: urban population growth, urban dedensification, economic growth and government policy. Additionally, the literature demonstrated that cloud geo-computing is increasing the efficiency with which ULE researchers can analyse urban footprint growth. The cloud geo-computing platform Google Earth Engine was used to analyse the urban extent of the City of Calgary over time. That data was merged into a time-series dataset that was utilised in a vector GIS environment to analyse the radial linear urban land expansion of the city between 1985 and 2020. The results showed that the city grew in a directionally non-uniform way and at different paces over each 5-year increment. This methodology constitutes an addition to the growing body of ULE research by providing a different perspective from the commonly used area-based ULE analyses.

Table of Contents

Introduction

This literature review is concerned with the principal drivers of urban land expansion (ULE) and the implication of cloud geo-computing for the quantitative measurement of ULE. ULE is a phenomenon that is presently occurring in almost all urban regions throughout the globe regardless of their development status. ULE is the process of urbanized land footprint expansion that results from the conversion of greenfield lands on the peripheries of cities into urbanized neighbourhoods or commercial districts. The rapid growth of cities throughout the world has increased concerns about the environmental, social and economic effects of ULE. The growing body of research on ULE has been particularly focused on East Asia because of the high rate of peri-urban land loss caused by the explosive pace of urbanisation in the last few decades. This period of explosive urban growth coincided with improvements in remote sensing technology and growing data libraries which enable time-series analysis. The literature elicits similar drivers of ULE globally to those described in the East Asia studies. The academic literature describes four primary drivers of ULE as we see it throughout the globe today: urban population growth, urban dedensification, economic growth and government policy.

Though it is difficult to disentangle exactly how much of an effect each of these four factors has had at a given time and place, researchers have measured the geographic urban land expansion of many cities throughout the globe using quantitative geographic methods and geospatial technologies. Much of the literature analyses ULE through case studies of specific urban regions or as ULE methods development on small geographic land samples. The scaling limitations of satellite data processing before the advent of cloud geo-computing limited the scope of quantitative ULE research because of data storage and processing constraints. An exploration of the quantitative ULE literature shows that it is quite methodologically

heterogenous, with researchers using spectral, algebraic and machine learning methods to measure or predict ULE. Geospatial methods have evolved quickly toward utilising satellite imagery to more efficiently model ULE in cloud-based geo-computation platforms. The literature suggests that cloud geo-computation is improving scalability in geospatial data sciences generally and quantitative ULE studies specifically.

The project that proceeds the literature review seeks to develop a spatial time-series based method for measuring the radial urban growth of Calgary, Alberta. Surveying the literature showed that the field lacks a radial linear growth metric. Almost all the reviewed research looks at areal urban land expansion (AULE) as the main metric of urban growth. This concentration in a single metrics category indicates that some alternative measurement schemes should be explored. Landsat images were used in the cloud geo-computing platform Google Earth Engine to create an evolutionary dataset of the urban footprint of the City of Calgary between 1985 and 2020 using spectral indices, in 5-year increments. With this data, a methodology for assessing linear urban land expansion (LULE) was developed using conventional GIS software. The results showed that Calgary had a rising annual average rate of LULE until 2015 and developed in a non-uniform way during the study period. A significant drop in the rate of ULE was noted between 2015 and 2020. However, this paper will not disentangle which of the four noted ULE drivers was the most impactful on Calgary's rate of LULE. The findings outlined the heterogenous nature of city growth both temporally and spatially using a possibly novel methodology.

Literature Review

In studying the academic literature on urban land expansion, four principal drivers emerged. These four drivers of urban land expansion are urban population growth, urban population dedensification, economic growth and government policy. Much of the research looks at the history of city-regions and the multifactorial characteristics of their emergence. The geographic pervasiveness of the ULE issue indicates that it is a global phenomenon.

City-regions throughout the globe are struggling today to counter the forces of low-density urban growth. Containing ULE would help reign in the negative environmental, fiscal, and social costs of unfettered urban land expansion to achieve more sustainable urban growth. To contextualize the project that follows this literature review, the four principal drivers of ULE will be discussed in the context of Calgary, Alberta.

The literature also highlighted that the advancement of new hardware-software system architectures puts the field on the verge of creating high-resolution ULE studies with a global scale. Research up to the recent adoption of cloud geo-computing is very methodologically heterogenous and limited in spatial extent. Improved scalability from the adoption of cloud geo-computing will drive a consolidation of ULE methods and lead to a clear and replicable set of ULE metrics for global and regional studies.

Four Primary Factors

Urban Population Growth

The literature suggest that urban population growth has been one of the primary drivers of the expansion of cities globally. Some researchers call this urbanization, which is a closely connected phenomena to ULE. Urbanization is broader in scope as it encompasses the wholistic and dynamic processes of both city building (fringe development, ULE) as well as urban transition and transformation (internal urban redevelopment). This definition characterizes the process of physical urbanization, whereby places are becoming progressively 'more urban' as urban land uses expand and intensify. However, urbanization is also commonly used as a term for demographic process where a greater proportion of global or local populations live in urban rather than rural places. This last definition explains why most scholars agree that modern urbanization began around the time of the industrial revolution. During that period, a large portion of rural populations were displaced or moved into cities in the United Kingdom. This rapid population urbanization would soon be followed by other major Western European and North American countries.

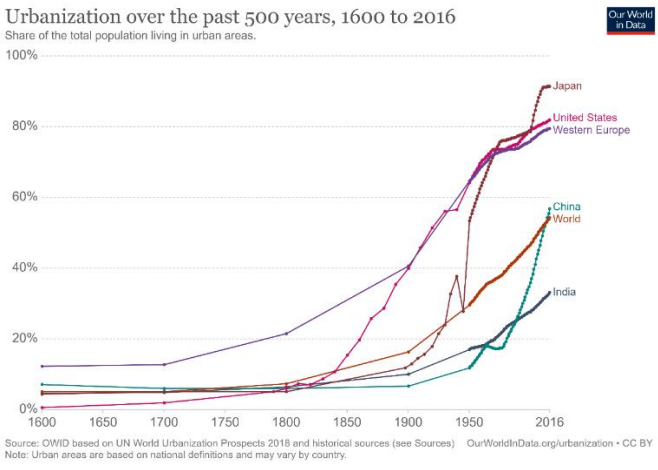

Figure 1. Urban population proportion over time in notable urbanizing countries (Global Change Data Lab - Oxford University, 2018)

Urbanization has driven up the proportion of the human population living in cities since the time of the industrial and agricultural revolutions of the late 18th century, which transformed population dynamics in a matter of about two generations (Global Change Data Lab - Oxford University, 2018). Today almost all countries throughout the world are experiencing some form of rapid or consistent population urbanization. Population urbanization helped the global urban population to surpass the rural population in mid-2009 for the first time in history (United Nations - DESA, 2009).

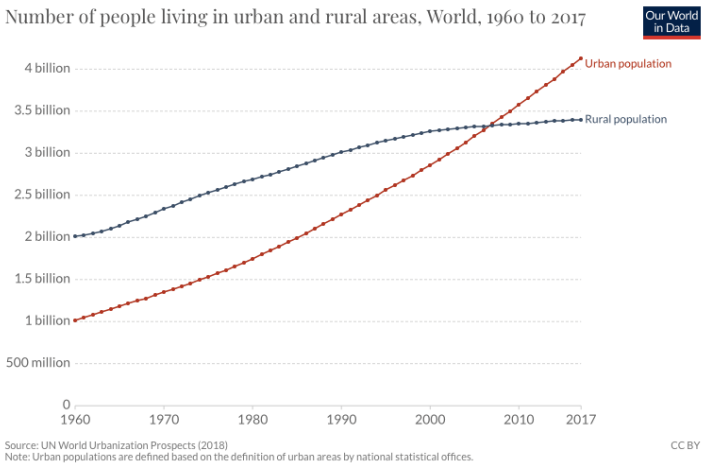

Figure 2. Graph of global urban and rural population over time (Ritchie, 2018)

Though some countries were later to begin their process of mass population urbanization, the process appears to be accelerated in nations that have urbanized in the post-war era. *Figure 1* shows that Japan and China have notably steep urbanization curves since the end of world war 2. India appears have a steepening curve that indicates mass urbanization is only just beginning in that country. The urbanization of the population of India will moved hundreds of millions of people into cities in the coming decades if the current trendline continues.

Much of the research that describes the drivers of ULE focuses on urban population growth in in less developed countries (LDCs). The pace and form of ULE can have a significant

effect on environmental, human, fiscal and infrastructural risks. Many less developed counties lack the resources or governing capacity to fully control or even direct urbanization, which often results in dangerous infrastructure and unserviceable neighbourhoods. This problem is aggravated by the fact that LDCs typically have higher rates of population growth. This results in unsustainable urban development which can perpetuate poverty, poor health and economic problems.

Cities like Port-au-Prince, Haiti are known for their sprawling completely unplanned and unserviced slums. The city was hard-hit by the 2010 Haiti Earthquake, which killed an estimated 315 000 people. The lack of building codes and poor zoning resulted in an enormous amount of building collapses when the earthquake struck (DesRoches, Comerio, Eberhard, Mooney, & Rix, 2011). Additionally, the unplanned and unmapped neighbourhoods with poor mobility made it very difficult to initiate first responders. This example demonstrates that uncontrolled urbanization can exacerbate disaster risks because urban disaster resilience is partially contingent on building cities that are physically resilient.

Another example of this is Dhaka, the capital of Bangladesh. Dhaka has been the focus of many studies on rapid urbanization in less developed countries because the city has experienced surging internal population growth and a concurrent movement of rural population to this major city. Dhaka, like much of Bangladesh, is at risk of flooding given that it is located on the enormous Ganges River Delta. To further exacerbate the human and infrastructure risks, new development appears to be encroaching on increasingly flood prone areas (Pramanik & Stathakis, 2015). Pramanik & Stathakis (2015) point out that land-scarcity is beginning to assert itself at a time when climate change is increasing the frequency and extent of floods.

The Oxford University Global Change Data Lab (2018) statistics presented in *figure 2* show that between 1975 and 2015 the proportion of the Chinese population that was urbanized increased from 17.4% to 55.5%. Using UN data (2019) to adjust for the change in total population over that time span, the urban population of China increased from 162 million to 750 million people in a span of 40 years. The incredible scale of development and land conversion required to achieve this feat likely represents one of the single largest landscape transformations in human history.

Contrast this with most developed countries, like Canada, where the process of urbanization has been in effect for well over a century. As a settler colonial state, the initial immigrant/settler population of Canada was made up primarily of rural homesteaders. At the turn of the 20th century, the population of Canada was 37% urban and 63% rural (Statistics Canada, 2018). By the 2018 national census, 71.5% of the Canadian population lived in a census metropolitan area (CMA), a proxy for a moderately sized or major urban center. Compare this to 1941, when only 54% of Canada's population was urban. The urbanization of the Canadian population has resulted from three separate dynamics: (1) migration of rural population to urban areas, (2) endemic population within cities and (3) foreign migrants choosing to settle mostly in major cities (Caron Malenfant, Milan, Charron, & Belanger, 2007).

Urban Dedensification

Throughout the academic literature that explains, analyses, and predicts ULE, urban population dedensification remains one of the most common themes. In public discourse, population growth is often erroneously claimed to be the main or only cause of urban land expansion (Wihbey, 2017), particularly in reference to less developed countries. Research shows that urban population dedensification is nearly as important of a factor as urban population growth in driving ULE. Literature on the subject by Günerlap et al (2019) showed that declining urban population density between 1970 and 2010 in most of the world was quantitatively of more importance in driving urban land expansion. This is illustrated most simply by their determination that the global urban land expansion rate held around 5% annually for the entire period, far exceeding the global population growth rate reported by the World Bank (2018), which was in a steady decline from 2% to 1.2% annually during the same 40-year timeframe. This dedensification phenomenon appears to be pervasive globally, regardless of the economic status of a country.

These authors showed that there is a direct relationship between urban population density and land conversion, particularly in North America, Europe, India and China, where urban population densities consistently declined during the study period. Their counterfactual analysis showed that during their 40-year study period, declining urban population density alone resulted in 125 000 square kilometers being converted into urban land globally. That represents the urbanization of an equivalent land mass to the State of Mississippi. The dedensification of cities is closely tied to economic growth, which allows a growing middle class to afford less densified and more comfortable housing. This was the case during the booming post-war Fordist period in

North America (Filion & Bunting, 2015) that saw the rising primacy of the automobile and low-density suburban housing.

A similar pattern of urban dedensification is occurring in China as their economy grows (Gao, Wei, Chen, & Chen, 2014). Günerlap et al (2019) determined that Chinese cities now develop land at a density of roughly half the new development density in 1970. The economic transformation of China is the ultimate case study of massive scale rapid urbanization. A significant body of work researches and analyses the growth of Chinese cities and the urbanization of the Chinese population in the span of less than 2 generations. On the macro-scale, urban population growth and falling development density cause urban land expansion. However, the lower-level driving factors that determine the forms of the urban land development span from geophysical to socio-economic. These smaller scale factors can ultimately determine the population density at which development occurs.

Looking at the literature on Africa, it appears that present urbanisation in Africa is characterized by expansive sprawl and declining urban population density (Dodman, Leck, Rusca, & Colenbrander, 2017). This is result of rapid population growth, economic change, inadequate infrastructure to support higher population densities and a lack of governance capacity and resources to implement functional urban planning. Dodman (2017) points out that between 1985 and 2000, Accra's urban land cover expanded at twice the rate of population growth, a similar metric to the aforementioned ULE of transitional China. Since then, population growth in sub-Saharan Africa has remained explosive. This highlights the concerning trend that cities are not developing in a way that holds or increases aggregate population density. This trend, which is at play in most medium to large African cities explains why sub-Sahara Africa is expected to have the highest rate of urbanization in the world for the coming decades. African

nations have a unique convergence of all four principal causes of ULE. Growth modelling by Angel (2011) predicted that urban lands would multiply twelvefold in Saharan Africa by 2050 relative to the 2000 geographic extent of urbanized land area.

It is possible, albeit rare to see development that increases the aggregate urban density of a city-region. One such example is Singapore, which has a unique style of closely managed development and housing market regulation that has allowed the middle class to flourish in a globalized city-state with hard physical limitations on land availability. Singapore was forced to focus on densification because of rather unique geographic, economic and social factors which are not in play for most other city-regions. As a result of these unique conditions, Singapore is urbanizing in a way that produces almost no ULE. Despite the existence of rare case studies like Singapore, unconstrained urban land expansion is the norm throughout the world rather than the exception, and unfettered ULE remains widespread.

Economic Growth

The literature suggests that economic growth is another driving factor of urban footprint growth. As cities have become the growth engines of service and manufacturing economies, they absorb more land and human capital from rural resource-oriented rural economies. Besides economic necessity, people also concentrate in cities to pursue economic opportunities associated with education, innovation, economic diversity, and the ability to specialize skills for niche industries. A prosperous urban economy also leads to the expansion of industrial land as businesses require more space for operations. Governments also perpetuate ULE by investing in public infrastructure to support the growing population and business activities. However, government projects are not necessarily correlated with economic growth because public infrastructure investment is used to stimulate a weak regional economy as well.

One of the most powerful examples of economic growth generating ULE is the economic growth period of China throughout recent decades. National and subnational governments were pivoting toward an economic growth orientation during this time. Economic reforms drove the transformation of the Chinese economy at least partially through the reorientation of sub-national governments toward a growth paradigm, which increased pressure to urbanize large amounts of rural land to generate regional economic growth and rents. Gao et al (2014) attempted to develop a conceptual framework for the analysis of land use change during China's famed economic transition. The context within which they operated was the so-called 'triple process': marketization, globalization and decentralization.

This process of political-economic reform is the result of all three 'processes' working in conjunction. (1) Economic globalization drove the necessity of seeking comparative geographic advantage to produce localized economic growth, (2) marketization meant economic and

political pressure mounted to develop land to its ‘full’ market-determined potential and (3) decentralization forced local-regional governments to pivot towards development and rent seeking behaviour in order to bolster public finances as the national/central government off-loaded tax collection and service provision functions on lower-level governments.

By approving or facilitating the development of large amounts of land, they were allowing the economy to grow and become spatially established in the previously agrarian countryside. Within the political-economic framework of their analysis, it is necessary to consider land as a resource and as such “land use reflects the most direct reaction of mutual influence and interaction between the humanistic and natural subsystems.” (Gao et al. 2014) In this way land development was a way for China to exploit its vast land resources. The urbanization of raw land can increase the economic productivity of a given unit of land. This occurs because urban economies are more compact which a greater output per nominal unit of land compared to diffuse agricultural and resource activities. This creates an undeniable economic incentive to urbanize peri-urban lands. However, that development simultaneously consumes agriculturally productive lands, which is an economic trade-off. Though economic growth from ULE far outstrips the loss of agricultural productivity, concerns about productive land loss are present throughout the literature on urban growth.

Globally, 60% of the land developed between 1970 and 2010 was formerly agriculturally productive (Günerlap et al, 2019). This outlines a potentially looming crisis of food security as many nations will begin to experience declining agricultural productivity due to climate change, in addition to having experienced irreversible land loss to cities over the preceding decades, which will exacerbate the problem. D’Amour et al (2016) determined that between 2000 and 2030, an aggregated 3.2% of global crop land will be lost to urbanization. However, land loss is

variable by region, with China, Vietnam and Pakistan losing between 5-10% of their productive crop lands during that 30-year period. Zhang et al (2017) did a case study on the Beijing-Tianjin-Hebei region to determine the extent of ecosystem services losses caused by ULE. For their analysis they considered food production, carbon storage, water retention and air purification as the four primary components of ecosystem services rendered. According to their analysis and forecast model, the urbanization of ecosystem services producing lands is the cause of upwards of 84% and possibly as much as 97% of total ecosystem service losses for the entire region between 2013 and 2040. This demonstrates to which point urbanization is an economic trade-off against agricultural and ecosystems services productivity.

Fully 80% of the predicted global loss is set to occur in Asia and Africa, continents that are developing at a rapid pace and have many associated growing pains (D'amour et al, 2016). The researchers did however note a compensatory effect where the globalized food system may help to soften the blow for countries that see the largest losses of productivity. They also noted that sub-Saharan African countries have a large agricultural productivity gap which could be closed by extensification (cropland expansion) and integrating agricultural technology and better land management to intensify use of existing croplands. However, this unexploited agricultural productivity does not exist in in South and Southeast Asia where almost all suitable land is already under intensified multi-crop cultivation.

In the Canadian context, the problem of high-productivity agricultural land loss is particularly acute because early settlements were located according to proximity to productive farmlands and waterways. As these settlements grew and eventually urbanized, they became modern Canadian cities that paved over some of the most productive agricultural lands in Canada (Statistics Canada, 2005). Fortunately, the forms of peripheral/suburban development have

evolved towards slightly higher density in many cities (Millward, 2008) as planning departments have had to acknowledge their fiduciary responsibility to taxpayers because very low-density development is a net fiscal drain on municipalities (Goodman, 2019). It is yet to be seen if a refocus on dense forms of development would be enough to reduce productive farmland consuming ULE.

Government Policy

The literature suggests that governments policy is one of the primary drivers of ULE because it dictates land management jurisdiction and high level housing policy that can stimulate the housing market. Despite this, government policy is simultaneously one of the most effective tools to control ULE. On a global scale, runaway urbanization is having a major impact on arable farmlands and natural areas as cities continue to expand their spatial footprint (Ali, 2008). For this reason, continual development on the peripheries of cities can have major implications for food security, regional biodiversity and disaster resilience (Tan, Li, Xie, & Lu, 2005). These are important considerations that can be effectively addressed by government policy.

Stelter and Artibise (1986) expounded on the political conditions that allowed North American cities to annex urban-rural fringe lands almost indefinitely through most of the 20th century. The appetite for annexation was high in the United States well before Canadian cities began booming around the turn of the 20th century. American cities had a significant lead on urban land expansion because of greater population numbers and earlier population of mid-western and western states. Central city governments and business interests were often on board with annexations because they believed that ‘bigger was better’. Independent surrounding communities were willing to be absorbed into the larger city’s political apparatus, typically in

exchange for reductions in taxes, improved civic infrastructure and in some cases to reduce the influence of a meddling local political class.

By pursuing large land annexations, American cities were able to somewhat set a precedent of how Canadian cities would access large quantities of developable land and peripheral communities into central cities. Canadian cities were quick to follow suit as soon as Canadian urban populations started booming. The formation of critical mass in cities was viewed as a way to assert regional dominance to attract additional population and economic growth. This virtuous cycle of growth and annexation was almost uniformly supported by civic and business leaders who were trying to engineer urban and economic growth. The cycle of urban growth and expansion was fuelled by political conditions that allowed cities to annex essentially unlimited quantities of greenfield lands into the jurisdiction.

Within the context of North American suburbanization and urban political systems, consolidation of city-regions through annexation was an important growth tool used to accelerate the provision of municipal services to suburbs in a way that was more cost effective than remaining self-supporting villages (McCarthy, 1986). Improvements in public infrastructure that accompanied annexations and tax reductions in the suburbs meant that North American cities were ripe for urban land expansion into greenfield lands. During this time, the single detached home increasingly found its place in North American culture, eventually to be touted as the illustrious ‘American Dream’.

McCarthy (1986) notes that the annexation paradigm shifted eventually. The major Canadian growth centers of the 19th and 20th centuries, Montreal, Toronto, Winnipeg and Vancouver have effectively ceased annexation in the modern era and become shut-in by surrounding suburban communities. These surrounding communities are now the primary source

of regional ULE for these city-regions that have opted to embrace the idea of metropolitan governments instead of annexation to facilitate regional cooperation and integration.

In some cases, greenbelting has emerged as a provincial/state level response to unfettered ULE and concerns about losses of highly productive agricultural lands. In Canada, the British Columbia and Ontario provincial governments have implemented greenbelts to reign in urban sprawl (Ali, 2008) in the Lower Fraser Valley and the Greater Toronto Area (GTA), respectively. Ali (2008) points out that thus far the land protections have worked in the GTA, however they have caused an unintended increase in the value of the existing housing stock by limiting the developable land supply. To prevent this market-effect, local governments would need to intensify land use of the existing urbanized area or insist on new developments being high-density to accommodate more population and meet housing demand with a smaller supply of land.

However, putting a dent in housing supply is not always the result of implementing greenbelts. In Seattle, the implementation of an urban growth boundary (UGB) improved housing affordability for low-income groups because the city administration allocated a greater portion of redevelopment permits to multi-family units (Ali, 2008). Such an initiative would also serve to re-densify the inner city, a stated goal of many modern planning departments and academics. Greenbelts have emerged as a practical response to ULE and present a contrast to the government policies that have accelerated ULE throughout the urban history of Canada. It is yet to be seen how resilient these policies are against the vested interests of land developers.

Housing policy is a tool leveraged by government to create economic growth by expanding demand for new housing. Government policy in Canada is used to encourage home ownership by facilitating mortgage loans through government-backed loan insurance, equity

sharing and tax incentives for homeowners. Pro-home ownership policies are a testament to the degree to which the Canadian economy is structured around land development, construction and the expansion of housing. However, peripheral urban development does respond to a market demand for lower density forms of housing and helps to accommodate a growing population. It is also worth pointing out that suburban neighbourhoods are well suited for families that prefer not to live in high-density housing and cannot afford low density residences in gentrified inner or mid-city neighbourhoods. Home ownership has also proven to be a useful tool for wealth creation in Canada, particularly for immigrant families that often come with little existing financial resources (Simone & Walks, 2019). Home ownership can also create strong communities because residents are personally invested in the long-term success of their neighbourhoods.

ULE in Alberta City-Regions

Population Growth. Population growth in Alberta has proven to be one of the highest in the nation, which has fuelled the spatial expansion of cities. The study area for the research that will follow this literature review is Calgary specifically, however the Edmonton-Calgary corridor is important in the Canadian population context. These twin cities are linked by a major economic and transportation corridor. The Edmonton-Calgary corridor has a population of over 3 million people, with 1 366 000 and 1 498 000 in the Edmonton and Calgary census regions (divisions #11 and #6) respectively. During the 1997-2001 inter-census period, Calgary experienced the most rapid growth in the nation with an increase of 15.8%, and Edmonton trailing with a considerable population increase of 8.7% (Statistics Canada, 2002). This population boom was thanks in part to a rapidly expanding oil and gas sector that was creating

large direct and indirect employment growth. To house this growing population, the City of Calgary expanded rapidly. It is perhaps for this reason that Edmonton and Calgary have somewhat of a reputation for having uncontrollable suburban growth.

The Edmonton-Calgary corridor is considered one of the four concentrated urban growth regions in Canada, with the other three being the extended Golden Horseshoe in southern Ontario, the Montreal region and the combined Lower Mainland and south Vancouver Island. Between the 1997 and 2001 national census, these four regions accounted for nearly all the population growth in Canada at 7.6%, while all other regions combined accounted for an almost negligible population growth of 0.5% (Statistics Canada, 2002). It is telling that the four major city-regions of Canada are essentially creating or absorbing all the population growth in Canada.

Urban Dedensification. Many cities are notorious for their unconstrained low-density suburbanization. North American cities have had a reputation for this since the post-war era ushered in massive scale suburbanization of cities. Low-density housing development on the peripheries of cities drove down the population density of north American cities and caused their urban footprints to expand significantly. The two major cities in Alberta, Edmonton and Calgary, both develop radially and swallow up enormous amounts of exurban, greenfield and agriculturally productive lands for low density residential and commercial developments. This suburban development is largely unconstrained by municipal planning departments that have rarely intervened to increase the density of proposed suburban developments. Furthermore, development is occurring at the fastest possible rate given market demand, with little regard for environmental, fiscal or social considerations. Though recently, the two cities have been working towards increasing density in mature and developing neighbourhoods (City of Edmonton, 2017)

to improve the net-negative fiscal effects that suburbs have on the municipal purse (Goodman, 2019).

Economic growth. Alberta has experienced rapid (albert fluctuating) economic growth, which has factored into the expansion of residential areas, industrial and retail centres, and public infrastructure to support the growing population and economic activity. The growth of the urban population and the dedensification of cities can also be viewed as a function of economic expansion and transition. As cities are the primary centres of economic activity in Canada, they draw in population seeking economic opportunities, which increases demand for housing. Additionally, the wealth created by the strong economy of a city becomes fuel for low-density housing development which can result in the dedensification of the city. As the middle class grew in Canada, so too did the demand for low density housing, particularly in the post-war era, which saw sustained economic growth and the emergence of seemingly limitless demand for family-oriented housing because of the baby boom after the World War II.

Beyond strictly looking at residential development led ULE, urban economic growth causes the expansion of commercial and industrial districts on the edge of cities, which is also an important contributor to ULE. Davies & Baxter (1997) explored the commercial composition of one of Calgary's major highway oriented commercial ribbons over a 30-year period via analysis methods derived from urban factorial ecology. Besides the analytic results of their study, they pointed out that the emergence of the highly land-inefficient urban form they call a highway-oriented ribbon was almost entirely codependent on the emergence of automobile-oriented suburbs in southern Calgary. The massive growth in the south of Calgary, which constituted almost 50% of the city's urban land growth during that epoch, drove a commensurate demand for concentrated roadside commercial, professional and retail services. This form of commercial

development is contrasted to older inner-city and downtown commercial districts because of the necessity for massive land-inefficient surface parking.

Though the Macleod Trail area lacked any comprehensive urban planning, the city administration did intervene to make sure large portions of land were allocated to surface parking, something that the city considered essential to ensure the success of the commercial district and prevent congestion from effecting MacLeod Trail directly. Though Macleod Trail represents only one case study, the development trend is clear in North America, these commercial and retail districts are part-and-parcel of residential suburbanization because they fulfill the consumer demand for services that are largely unavailable in residential-only neighbourhoods. This urban development modality builds on the land-inefficient trend of modern urbanization that is oriented around consumerism and the primacy of the personal automobile. This example also outlines the extent to which land inefficient commercial districts and residential development prompted by economic growth contribute to ULE.

Government Policy. Edmonton and Calgary have continued to expand their urbanized footprints and legal city limits in the modern era as suburban growth very much remains the development paradigm on the western Canadian prairies. This is somewhat unique compared to the other major city-regions in Canada, which McCarthy (1986) described as having central cities shut-in by outlying independent suburban communities. Edmonton is partially shut-in by the suburban communities of St. Albert, Sherwood park and the Enoch Cree Nation Reserve but continues to pursue annexations of surrounding county lands. The 2019 annexation of lands up to Beaumont city limits and the northern edge of the Edmonton International Airport demonstrate that the city administration has continued to pursue expansion of their developable land supply. The periphery of Calgary is almost entirely available for annexation as needed for development,

other than the Tsuu T'ina Nation Reserve which borders the central-west section of the city. Calgary has consistently annexed new lands as needed for the development of low-density suburbs.

Cities in Alberta have also likely had ULE driven by federal housing policies that encourage home ownership. Examples of this include the Home Buyers Plan which allows home purchasers to access retirement savings for a down payment, CMHC mortgage insurance that helps banks insure mortgages (thereby incentivizing lending) and the newly minted First-Time Home Buyer Incentive through which the CMHC take on an equity share in the purchase (Canadian Mortage and Housing Corporation, 2019). Though we will not speculate on the effectiveness of these measures, they have likely had some macroeconomic impact on the Canadian housing market and in Calgary as well.

Local government planning also has an impact on ULE. Municipal and provincial governments invest in public infrastructures that facilitate the geographic expansion of cities. The Anthony Henday and Stoney Trail ring roads are examples of this. These road and utility corridors were decades in the making and will facilitate the expansion of the cities for decades to come. In both cases suburban development has already 'jumped' the corridors as neighbourhoods have sprung-up outside of the ring roads. These corridors are roughly half a kilometer wide, which directly expanded the cities. They are also facilitating the secondary expansion of the cities by facilitating commuting from the suburbs and providing enhanced mobility for economic activities.

Qualitative ULE Methods

Though the literature has outlined 4 principal drivers of ULE, very few researchers try to disentangle to what degree each of the drivers is operative for a given urban region at given time. Because of the individual complexity and the way in which these factors interact with one another, factor analysis of ULE drivers is incredibly difficult and beyond the scope of this project. The aim of this section is to delve into existing methods of ULE measurement and forecasting to attain a better understanding of why only incremental methodological improvement has occurred in the field up until recently, and why cloud geo-computing represents a shift in how geospatial researchers can measure aggregate ULE.

ULE Modelling

Data Sources. There are three common data sources that are typically used to identify the built-up extent of cities. These three data sources are remotely sensed images, vector geospatial data and spatialized census data.

The first and foremost data type is remotely sensed images, which can be classified using various spectral, statistical or machine learning based methodologies. Remotely sensed spectral signatures, typically in the visual or near-visual spectrum, are expressed as pixel values and used to identify the extent of urbanization in a city-region using image classification software. This method was successfully deployed by Pramanik & Stathakis (2015) using open-access Landsat imagery to identify the urbanized land area of Dhaka, Bangladesh. They pointed out that using satellite imagery was well suited to their research because the Dhaka city-region lacks formalized planning to control, direct or measure the rapid urban footprint growth that is occurring. This procedure requires minimal input datasets which are typically sourced from

reliable national satellite imagery databanks and not local authorities or city/regional governments, which often do not have these types of data available.

The NASA/USGS Landsat program is one of the leading earth observation programs, with data going back to 1972 when Landsat 1 was launched. The United States Geological Survey (USGS) directly disseminates Landsat imagery for free via its EarthExplorer interface. However, the volume of data in Landsat image tiles can be problematic for desktop hardware configurations, particularly if researchers are working with a multi-tile sized study area. Cloud computing has recently helped researchers overcome this scaling limitation. By storing the entire multi-petabyte Landsat archive at data centers, along with many other RS imagery collections and spatial datasets, researchers can program intensive data processing tasks to be performed at the data centers and subsequently download only post-processed or simplified output datasets.

Secondly, vector-based geospatial datasets from municipal archives, property zoning or surveying databanks can be used to identify developed properties as well as undeveloped lands within city limits. In many cases cities annex fringe land decades ahead of development, which means that the properties slatted for future development are within the city administrations jurisdiction long before being urbanized. These data sets have a high fidelity because cities typically maintain them on an ongoing basis as land-use evolves spatially within city limits. These types of high-value datasets exist as a result of tightly managed permitting processes and therefore are more available where planning departments are well established with GIS enabled data-systems. In other words, extensive urban vector datasets are more commonly available from city/regional administrations in developed countries with long-established systems of urban planning and histories of government-led land management.

Many city-regions in developing countries are trying to close the GIS capacity gap because of the necessity of better planning for sustainable urban growth as well as ensuring cities are well oriented towards economic growth, as it becomes apparent that cities are going to be the major economic drivers of the 21st century. However, it is difficult to build out high-quality vector and surveyed datasets retroactively, because of the high capital and labour cost of the effort as well as the difficulty of getting buy-in from stakeholders who are used to the status quo of loose zoning and land management. More established government GIS departments can keep their costs down by maintaining and updating vector dataset on an ongoing basis as internal redevelopment and fringe city building occurs.

Vector datasets can also be obtained from non-governmental geospatial data banks. These are usually the post-processed data products from the image classification process described in the above remote sensing section. Because of how commonplace and low-cost the process of image classification is, there are many ready-for-use classified vector data and map products available. However, a lack of standard classification practices and data crunching parameters means these can have varying fidelity, resolution and the input layers can be quickly outdated by the pace of new data production and physical landscape changes. Recent research by Liu et al (2018) demonstrated that the accuracy and resolution of five ready-for-use global-scale urban land extent vector datasets varied wildly and attempted to create a higher resolution product using cutting edge software-hardware architectures.

Lastly, spatialized census data can be used to identify tracts of land with higher population densities, which would indicate urbanization. With census data, the granularity can become important as most of the data is spatially aggregated to achieve mandated levels of anonymity on a scalar basis. Multi-level census data has reduced demographic datapoints as you

approach smaller census tracts. Conversely, as tracts become larger, data aggregation can cause spatial distortion in terms of value distributions. For example, a large census tract could be spatially made up of 75% unpopulated greenfield land and 25% high-density residential in the real world, but the aggregated data for that polygon would represent a low population density for the census tract because of spatial averaging. The way that census tracts are determined and spatially modified over time can also cause issues with data continuity and interfere with time-series analysis methods that require input spatial data to remain constant over the analysis periods. However, in some cases creative data aggregation and interpolation can be used to overcome this deficiency of spatial census data.

Remote Sensing Basics. Because Remote Sensing (RS) is one of the most powerful, reproducible, widely used method for urban land detection. RS data will be used for the modeling project that follows this literature review. Since the early days of remote sensing, it has been used as a tool for identifying the impact of human development on the surface of the earth. Early satellite images changed society's perception of our ability to impact our planetary ecosystem by showing the global geophysical extent of human development for the first time. The ever-growing open-source cataloging of remotely sensed images has become a powerful tool for not only instantaneous geographic measurements, but also temporal change measurement. The capacity for time-series analysis is improving as databanks now have considerable temporal depth and new images are added consistently.

Spatial Modeling. Determining the extent to which ULE transformed significant amounts of land globally or regionally is a worthwhile endeavour because the trend is clear that ULE will continue to occur as the modern development roadmap remains firmly entrenched in most parts of the world. Many methods have been applied to determine the extent of urban land

footprints, but none as much as the classification of remotely sensed satellite imagery. Remotely sensed image archives have become more accessible, temporally richer and image resolutions have improved as instruments have been upgraded. GIS has been used to model the urbanized footprint of cities since its inception, however the technologies that merge RS raster images with traditionally vector-based GIS platforms have caused somewhat of a consolidation of the two fields. Combining the strong suits of GIS and image classification allows geospatial researchers to analyze these rich datasets. Much of the value of the data comes from the temporality of the datasets, which allows researchers to perform time-series analysis.

Spatial Forecasting. From modeling and historical data, some researchers have attempted to create ULE forecasts. Spatial forecasting is a challenging task that typically requires temporally rich datasets and careful model calibration and/or parameterization. The development of more advanced urban growth modeling methodologies coincided with advances in geographic information sciences and remote sensing and data storage technology (Pramanik & Stathakis, 2015). A plethora of urban growth modeling methodologies now exist that explore various aspects of urban transformation and ULE. Those same researchers pointed to other significant research that used artificial neural networks, statistical models, multi-agent models and fractal models to analyse and predict ULE.

Cellular Automata. Among the urban growth modeling methodologies that Pramanik & Stathakis outlined, they chose to utilize a self-modifying cellular automata model in their ULE forecast of Dhaka. They argued that among these dynamic models, cellular automata were the strongest because of their close developmental ties to remote sensing and geographic information systems. Cellular models are spatially constructed from grids of raster cells. These raster cells can have values ranging from discrete or dynamic identifiers. Simple binaries can denote the

potential of a cell for future development (e.g. 1 = developable greenfield, 0 = undevelopable waterbody) and dynamic identifiers can be used to build out more detailed data. The dynamic identifiers can outline suitability or probability-based metrics of developability. For example, cells could be identified according to their average terrain slope. This datapoint could be used by researchers or urban planners trying to build out algorithms that allow certain types of land development within a specified slope range.

Spatio-Physical Limits and Stimulants. Developing limitation parameters on a spatial forecast model is important for producing accurate and credible forecasting because not accounting for heterogenous geographic factors would constitute a major oversight. In order to develop their forecast for the City of Dhaka, Pramanik & Stathakis (2015) input spatial datasets into the SLEUTH modeling software developed by Project Gigalopolis. Clarke (2000) hypothesized that "[urban settlements are] intensely impacting land, atmospheric, and hydrologic resources, urban dynamics has now surpassed the regional scale of megalopolis and must now be considered as a continental and global scale phenomenon". The acronym SLEUTH is used to identify factors that influence the location and pace of land development: slope, land-use, exclusion, urban extension, transportation and hillshade model. Their system includes transportation infrastructure in the model inputs because of the observable importance of connectivity to development, whereby higher connectivity equates to higher priority in urban development sequencing.

Global ULE Forecast. Angel et al (2011) developed a global ULE forecast for the period 2000-2050. To achieve a global full coverage forecast they used the Mod500 global urban land cover dataset which at the time was the "best of eight satellite-based global maps of urban land cover". Liu et al (2018) would later create an urban land-use classification methodology that was

globally scalable and drove the resolution up to 30m (NUACI – Landsat 5 TM TOA reflectance) from 500m per pixel (Mod500/Modis 500m). The global forecast that Angel et al (2011) developed showed that in the medium urbanization case, urban land cover in developing countries would increase from 300 000 square kilometers in the year 2000 to 1 200 000 in 2050, a threefold increase.

To predict the rate of global ULE rates, these authors relied on previous research that used geospatial methods to determine the historical rate of urban density decline by region on a global scale (Angel S. , Parent, Civco, & Blei, 2010). That research informed their low, medium and high annual urban density decline cases, which were 0%, 1% and 2% respectively. The authors pointed out that of the three cases, the high case was the global average from 1990 to 2000, the medium case was the long-term global average from the twentieth century and the low case of 0% density decline was observed in the United States throughout the 1990s. This points to the likelihood that the high urban land growth case would come to fruition based on the current global trend of dedensification outside of fully developed economies.

Cloud Geo-computation

Google Earth Engine. As a computational task, the analysis of remotely sensed images on a large scale requires powerful computers for data crunching and lots of memory to host the enormous quantities of pixel data remotely sensed images. As the number of satellites, frequency of image capture and resolution of remote sensing instruments have increased consistently, so too have the requirement to have more powerful computers to extract the maximum value from the datasets. Recently, the capacity problem of the desktop workstation configuration has been circumnavigated by innovations in cloud computing, particularly at Google Earth.

Google Earth Engine (GEE) is a free command-based platform for researchers to use cloud computing to access the extensive library of satellite data housed at Google Earth data centers and harness their parallel processing infrastructure. GEE can be used to perform analyses that are simply not possible on stand alone desktop workstations. Though global scale analyses existed previously, such as Angel et al (2011), this technology has given rise to the possibility of global scale analysis at high spatial resolutions.

Google Earth Engine offers an Application Programing Interface (API) that utilises the Javascript programming language for writing command line scripts to be processed at Google data centres. The API is the native platform for accessing GEE, but for users who are more fluent in Python, an Earth Engine API is installed by default in the Python-based Google Colab (Colaboratory), which is a Google hosted version of the open-source project Jupyter Notebooks.

Machine Learning/AI. It is important to distinguish between land-cover and land-use. Land-cover is the less complicated of the two, given that it can be obtained simply by analysis of the spectral signature of individual pixels. Analysing land-cover determines the composition of the surface material (e.g. forest canopy, pavement, grassland, waterbody, etc). By contrast, land-use accounts for the broader context of land-cover (surface material), but also how it relates spatially to other materials and the spatial arrangement/geometry of the objects themselves (Vernburg, van de Steeg, Veldkamp, & Willemen, 2009) in order to determine more specific, use-based classifications. For example, a pixel could have a land-cover classification of forest but be in an inner-city park. The greater context of land-use would capture the spatial properties surrounding the forest pixel and classify the land-use of this pixel as urban or be precise enough to classify it as a park. In *figure 3*, it is virtually impossible to determine the land-use feature (road) according to the spectral signatures of the pixels alone.

Figure 1. Land-use is difficult to determine according to pixel signatures (left), more complex image recognition is required. (Google Earth, 2019)

The process of determining land-use is computationally intensive and relies on complex predictive models, such as deep learning/deep neural networks (DNN). The utilisation of cloud computing can address the problem of computational intensity, which explains why much recent research relying on land-use classification merges the cloud computing of GEE with the Machine Learning protocols built into the TensorFlow software library, which some have called the Earth Engine of machine learning.

Cloud Geo-computing. Early research by Hansen et al (2013) in geospatial cloud computing demonstrated that the Google's data centre infrastructure could be harnessed to make the first comprehensive global assessment of decadal forest cover change (2000-2012) at a high resolution of 30 meters. Given current hardware constraints on desktop-based geo-computation, it was previously impossible for researchers to do this level of analysis. Though the project concept and principles of image analysis are straightforward, no researchers had yet been able to do high-resolution forest cover analysis at more than a sample scale. The alternative was also possible, global coverage albeit at a low spatial resolution.

The importance of being able to do global high-resolution analysis without field researchers or support provided by government organizations can hardly be overstated. Hansen et al (2013) pointed out that among the nations their analysis highlighted as experiencing intense forest cover loss, only Brazil provided annual data for forest cover change. Political and

economic motivations are standing in the way of many governments creating and releasing data that would incriminate them as abetting large-scale forest loss or other environmental degradation. Though that research did not look at ULE, the methodology applied is very close to what would be used to measure urban land change over time. The primary distinction is that different spectral signatures will be used to different types of landscapes.

The capacity to do large scale and high-resolution image analysis constitutes a paradigm shift in geospatial research. The availability of cloud geo-computing applications to researchers will also likely drive a consolidation of the heterogenous methodologies used in ULE research. Unfortunately, the ULE field appears to lack formalization or standardization that would allow the results of ULE studies to be more easily incorporated into discourses about land loss and urbanization controls. As the field matures, more standardized metrics will emerge. The addition of this new technology should accelerate that maturation and result in more efficient and enlightening ULE research. This combined with the integration with machine learning based image recognition will allow researchers to move beyond spectral based models.

Project Description

This project seeks to determine the pace at which linear ULE has occurred over time in the City of Calgary region, which is well known for unfettered suburban development. A combined remotely sensed image archive classification and GIS-based spatio-temporal analysis methodology will be applied to observe the pattern of linear outward growth of Calgary and the pace at which this outward movement is accelerating, decelerating or stable over time. This information about the change of linear outward growth is rather unique in that few researchers have approached the urban land expansion problem from the linear, rather than surface areal standpoint.

The goal of this research is to develop a methodology for determining linear ULE (LULE), breaking for the norm of using surficial/areal ULE measurement of urban sprawl. This research is using the cloud computing platform Google Earth Engine for data access and image classification before migrating into conventional GIS software (ArcGIS Pro) for vector-based time-series analysis. The relevance of this research is that the method provides a smaller-scale and more nuanced analysis, whereby individual plots of raw lands can be considered in terms of time-to-development. Surficial measurement and forecasting are more useful for calculating aggregate lands loss, which is relevant to research contexts such as arable lands loss.

This research will provide insight into the possibility of measuring the linear outward rate of ULE, using Calgary as a case study. The LULE metric could inform development planning and give prospective land developers and investors an understanding of the amount of time it would take to see a capital return on their land investment. This type of information could be applicable to urban and regional planning as well a business decision making.

Methods

Data Access & Preparation

The base data used for this project was acquired from the Landsat Tier 1 ("T1") image collection. The USGS preprocesses data to remove some of the complex data cleaning, refining and classification workload from researchers. Several different preprocessing methodologies are applied to the raw satellite images, which results in the publication of a range of data tiers and spectral information formats. Tier 1 data was selected because "Landsat scenes with the highest available data quality are placed into Tier 1 and are considered suitable for time-series analysis." (United States Geological Survey, 2018)

Within the issued T1 collections, the Surface Reflectance (T1_SR) dataset was chosen for each of Landsat 5, 7 and 8. Note that there is no Landsat 6 because in 1993 the satellite failed to reach orbit when its fuel-engine connection failed, preventing it from maintaining altitude (NASA, 2020). Fortunately, Landsat 5 remained operational well beyond its estimated lifetime, preventing the expected data gap when L6 crashed out of orbit.

Surface reflectance images are most suitable for this research because the data is atmospherically calibrated to display the true reflectance of the surface of the earth (L3Harris Geospatial, 2013), which is ideal for identifying land cover types according to their discrete spectral reflectance characteristics. All other ancillary vector datasets were constructed from scratch in Google Earth Engine or ArcGIS Pro or acquired from municipal and provincial open data banks.

Filtering & Mosaicking Image Collections

Image collections were separately filtered to create one dataset every five years between 1985 and 2020. These filtered collections were inclusive of image panes from a +/- one-year timeframe (3 years total). The 2020 dataset included all 2019 data in its date inclusion range through to Oct 02, 2020. 1985/1990/1995, 2000/2005/2010 and 2015/2020 were obtained respectively from Landsat 5, 7 and 8 based on which satellite was operational at the time. Across these three satellite image collections, the data has consistent formatting, encoding and resolution, meaning that all the javascripts used to access and prepare the first dataset were easily replicable across all the periods. Additionally, clouds and cloud shadows are labelled in a pixel quality ("pixel_qa") band which was used for pixel masking. A central point coordinate was used near downtown Calgary to create circular polygon with a 40-kilometer radius and collections were mosaiced and clipped to this geographic extent.

Indexing and Band Analysis

The Built-Up Index (BUI) method proposed by Zha et al (2003) and later retested by He et al (2010) was used. This approach relies on the algebraic fusion of NDVI and NDBI indexes and results in a "semi-automatic" segmentation because the resulting final dataset is a binary BUI raster layer, with the two binary classes being urban or non-urban land cover. The band math to achieve this exploits the differences in surface reflectance between red, near infrared and short-wave infrared for vegetated and impervious surfaces. The band math is as follows:

$$NDVI_c = \frac{NIR-Red}{NIR+Red} \quad (1)$$

Firstly, a normalized difference vegetation index (NDVI) is calculated for the study area and inputted as a new band called "NDVIc". Where c represents the continuous format of DN

values. Because Landsat has a relatively high resolution (30m), a low-pass 5x5 convolution filter was applied on the NDVIc band to remove outlying high-frequency values and smooth the images.

$$NDBI_c = \frac{SWIR-NIR}{SWIR+NIR} \quad (2)$$

Secondly, the normalized different built-up index (NDBI) was computed as an additional band for the study area. The band was convolved with the same 5x5 low-pass filter to smooth out the DN values.

In order to recode to continuous NDVI and NDBI indexes into binaries, DN thresholds needed to be determined for segmentation. The binary attribute represents the discrete urban land extent for each image. Vector sample sites were established for different land-cover types and histograms were analysed to determine optimal thresholds for the binary separation of urban and non-urban land according to the spatial distribution of DN values. Sample sites consisted of 4 roughly equal sized polygons that covered residential, industrial, agriculture and forest. The residential and industrial samples were combined to create an urban land sample and the agriculture and forest polygons were combined to create the non-urban land sample.

Firstly, histograms were generated for before and after convolution to determine if this approach was effective and necessary. Histogram DNs were counted according to the pixel content of the two combined sample sites. Results showed the convolution method was effective in improving land cover distinguishability withing the histogram distributions, see figures 7 – 8. Analysis of the convoluted DN histograms for the 2015 dataset was then used to determine an appropriate threshold for recoding the NDVIc into a binary NDVIb layer where 0 = urban and 1 = non-urban. The same process of threshold determination was repeated for the NDBI band by

viewing histogram DN distributions. The NDBIc was then also recoded into a binary band as NDBIb where DNs were valued at 0 = non-urban and 1 = urban.

When this process was repeated for the other images it became apparent that the DN thresholds determined by the initial 2015 sampling could not be reused for all the composite images because of spectral variations for the different datasets. This was likely due to seasonality in the remotely sensed data. This occurs because not all pixels are captured at the same point in the vegetation growth cycle because Landsat captures images only every 16 days. The histograms were viewed for each period to determine a starting DN threshold that was manually calibrated by the analyst using the RGB image as an underlay and the binary layers as an overlay. The calibrated DN thresholds for each dataset are found in *table 1* in the results section.

$$BUI_b = NDBI_b - NDVI_b \quad (3)$$

The BUIb band was calculated by subtracting the NDVIb band from the NDBIb band. The combination of these two datasets helped further enhance the classification power of the band math by increasing the data contrast between vegetation and impervious surfaces. The enhancement effect is a result of NDVI and NDBI capturing the opposite land cover types, but with different effectiveness. By fusing these two classifiers, the NDVI which is very accurate, sets a spatial limitation on the NBDI band which typically overestimates urban land. Some of this discrepancy in effectiveness is surely because a greenest pixel composite was used, which favours the application of normalized difference vegetation classification.

The raster images were exported as multiband geotiff files into google drive and subsequently migrated into ArcGIS Pro catalog. Each of the 8 study periods had 2 images of the study area. The two image exports were (1) an unconvoluted multiband RGB image for visual reference purposes and (2) a single band BUIb raster image. Additionally, the YYC centroid

points used for developing the study area buffers were exported to assist with the creation of ancillary spatial datasets for the spatial time-series analysis in ArcGIS.

ULE Data Vectorization and Editing

Each of the 8 BUIb raster images were converted to polygons using the Raster to Polygon tool. Polygons with a size less than or equal to 25 hectares were deleted by applying Select by Attribute and deleting according to the selection. The same process was repeated to delete polygons where the BUIb score was not equal to 1. The Aggregate Polygons tool was used to simplify and consolidate the polygons (parameters: aggregation distance = 1km, minimum area = 25ha and min hole size = 75ha). The resulting aggregated polygons were visually inspected for errors of omission and the pre-aggregated dataset was manually edited and reaggregated to solve for the errors in the 2020 dataset.

Parks and open space shapefiles were collected for major communities in the study area and fused into a single feature class (Town of Okotoks, 2020) (Town of Cochrane, 2020) (City of Airdrie, 2018) (City of Chestermere, 2020) (City of Calgary, 2020) (City of Edmonton, 2019) (Government of Alberta, 2017). The merged parks and open spaces polygons were clipped from the aggregated 2020 polygon to exclude parks areas. The parks deletion process only needed to be performed on the 2020 dataset as it would be inadvertently incorporated into all earlier datasets through clipping. Each dataset was clipped (Clip tool) according to the UL extent of the five-year newer UL extent polygon. This action was performed to cut down on spatial errors of commission based to the assumption that if a piece of land is undeveloped in the 5-years newer dataset, it would have been undeveloped in all earlier study periods as well. Each of the pre-2020

images were (1) thinned (BUIb = 1, Hectares > 25), (2) aggregated and (3) clipped to the extent of the next newest study period.

The earliest (1985) dataset was manually verified and edited to maximize fidelity. After the final manual editing, it was reaggregated and the regional parks file was clipped again to ensure edits did not overlap the parks omissions. From 1985 forward, each dataset was (1) merged into the next newest dataset and the new dataset was (2) dissolved to remove concurrent polygons. This action ensured that there were no instances that represented degrowth, which would have been an error of omission, based to the assumption that if a plot of land was classified as urban 5 years earlier, it would have remained urbanized in all following datasets.

Radial Polyline Fan

The following is the multi-step process to produce a 360-degree radial polyline fan with a 40-kilometer extent around the study area centroid point. A 40-kilometer polygon around the centroid points was created using the Buffer tool. The Feature to Line tool was used to generate a circular polyline on the buffer perimeter. An empty feature class was created in the project geodatabase to house the 360 radial endpoints. Within the Editor window the Create Features mode was applied to the empty feature class. The Create Points Along Line tool was parameterized to create 359 points plus an additional point at the start of the polyline. The Add XY Coordinates tool was used to put the point coordinates into the attribute table of the radial points and centroid points feature classes. The XY coordinates from the centroids were pasted as a second set of XYs into the attributes table of the radial points. The XY to Line Tool was used on the radial point attribute table. This created a new feature class that is made up of 360

polylines between the centroid point and each radial endpoint. Each line was assigned a degrees attribute between 1 and 360

It was deemed important to include Calgary adjacent communities in the analysis. The 40-kilometer distance of the buffer was chosen to include Okotoks in the region. This included Airdrie, Cochrane, Chestermere and Okotoks, which have a combined population of over 145000. These communities have a suburban character and like Calgary are expanding at a rapid pace. Because of their proximity, it is worth including them in the analysis because they are part of a connected city-region.

Time-Series Dataset

The extent of each individual dataset was erased according to the extent of the 5-year earlier dataset to isolate only polygons that represented growth over the intervening 5-years. The polygons in each dataset were collapsed into a single multipart feature using the Dissolve Boundaries tool. An attribute was added to identify the polygon year of origin and the 8 datasets were merged into a single ULE dataset. The Identity tool was used to parse each 40-kilometer radial line into 9 separate multipart lines for each sample year. Identification created a total line length (meters) attribute for each of the 5-year expansion lines. The tables were pivoted using the line degree ID as the pivot field to object length for each 5-year period as the data to be pivoted.

Results

Data Access + Preparation

Image collections were selected, time-framed, cloud/cloud shadow masked, mosaiced and geographically clipped to create the study area layers in *Figure 4* below. This is the resulting preliminary dataset in visual spectrum (RGB) format, but it contains may other bands that are not parameterized for display.

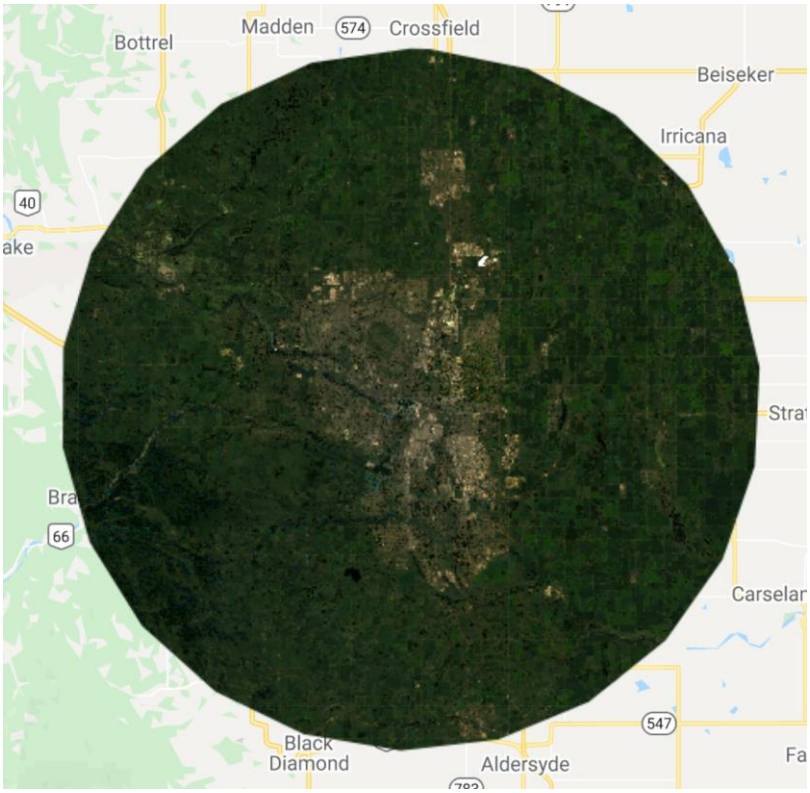

Figure 2. Study area dataset (2015) displayed in RGB format. 40-kilometer radial region for Calgary. Screen capture from the Google Earth Engine user interface.

Sample sites were prepared for testing and calibration throughout the iterative processes to follow. Two categories of sample sites were taken for four land cover types: residential, industrial, agricultural and forest. Histograms were plotted for the near infrared, red, green, blue digital number (DN) counts.

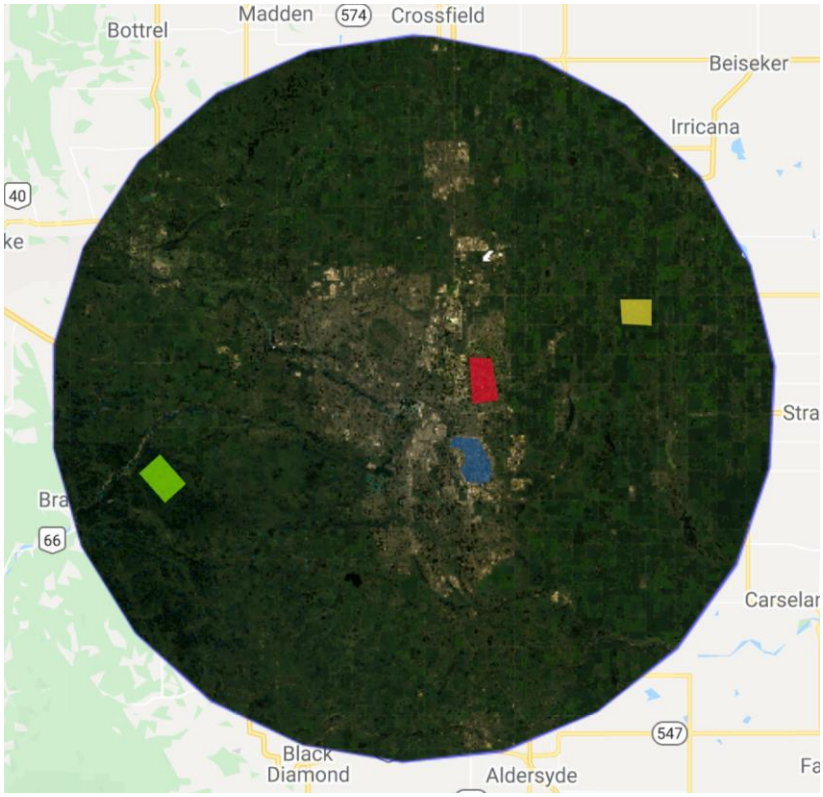

Figure 3. Sample sites for different land cover types. red=residential, blue=industrial, green=forest, yellow=agricultural.

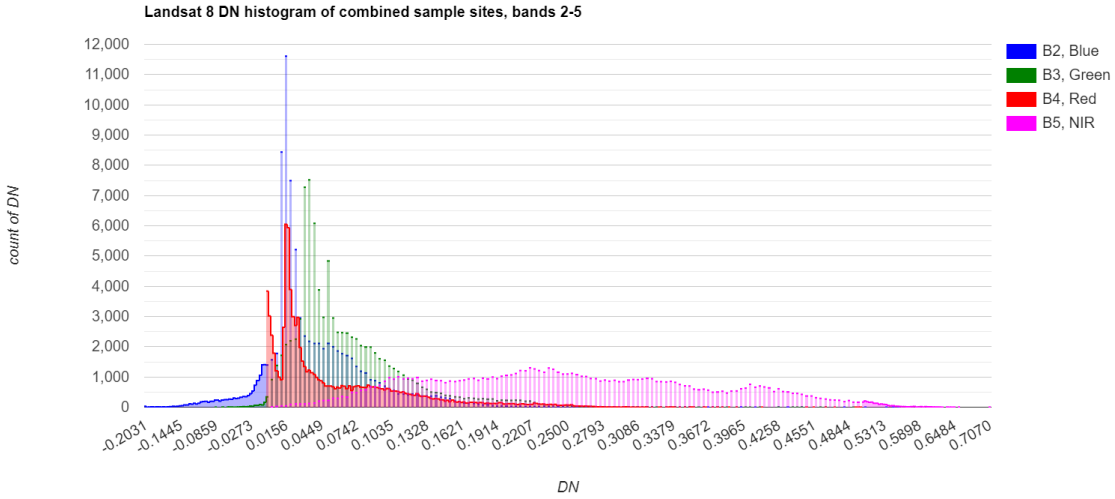

Figure 4. Histogram of visual spectrum plus near infrared digital number (DN) counts. Differences in spectral outputs for different surface types can be exploited to automate image classification.

NDVI band + Binary Threshold

Urban land. By observing the three following histograms it is apparent that non-urban land typically has NDVI values above 0.7, with a major inflection point at 0.85 (figure 7). The mixed composition of urban land makes the NDVI values significantly more spread out relative to the non-urban lands sample. Some of the higher values (see figure 7) could be characterized as cross sampling. This cross sampling occurs where trees are present in residential areas or a road cuts through an agricultural area, for example.

Non-Urban Land. The histograms show that non-urban (agriculture and forest) land is most spectrally expressive in the -1.6 to -1.3 segment of the histogram. Residential occupies the center segment and industrial lands is most expressed above -0.5. There remain some overlapping values across the samples, however these are mostly representative of places where the sample sites contain small segments of the other land cover types (e.g. small greenspace in a residential neighborhood). Smoothing will reduce this effect.

Data Convolution. The cross-sampled data was softened by running a kriging/convolution filter over the image to blend outlying pixel values using a low-pass filter. The convoluted histograms (figures 7-8) show that applying the low-pass filter was an effective tactic for concentrating DN values within their respective sample-appropriate ranges. The overlap between DN values in the 0.7 to 0.8 range was reduced by the convolution and it seems appropriate to assign a binary data splitting threshold at NDVI = 0.7. This threshold was applied as a binary classifier and the pre- and post-convolution images are shown in figure 9.

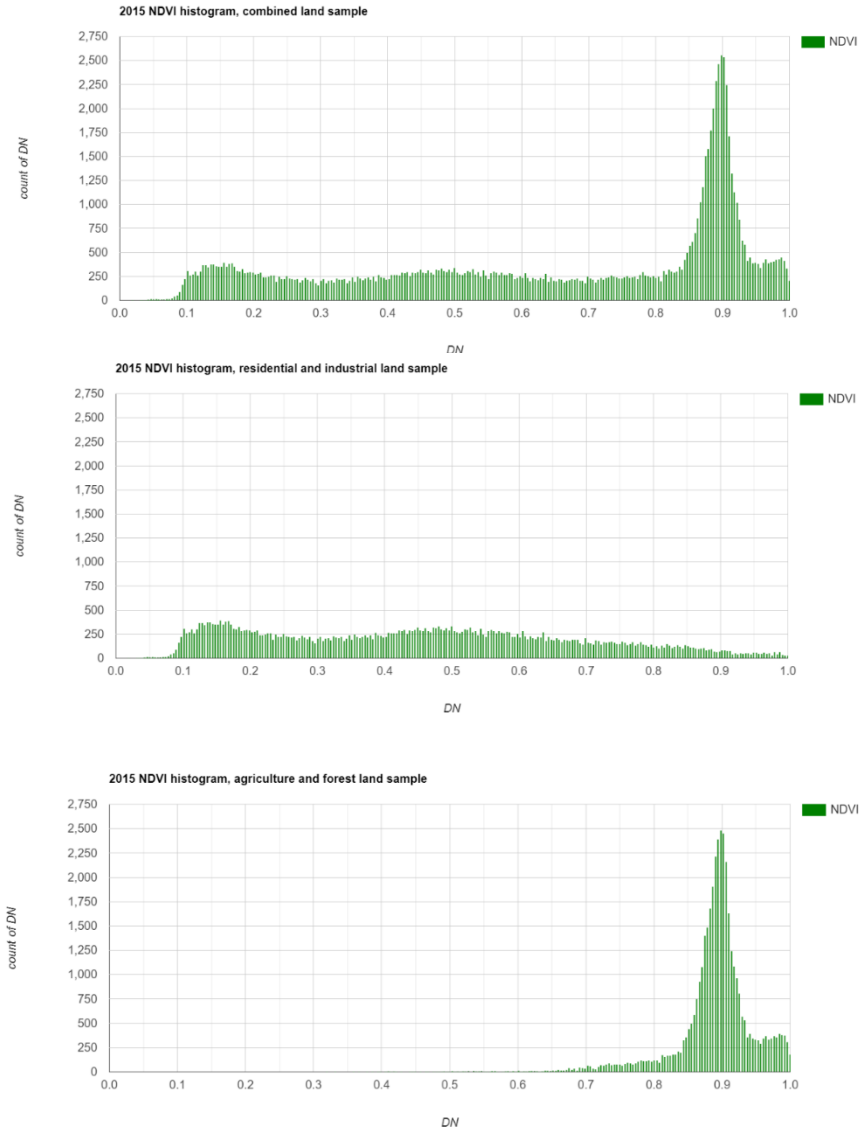

Figure 5 (3 vertical). NDVI histograms of unconvoluted samples in combined and separated formats.

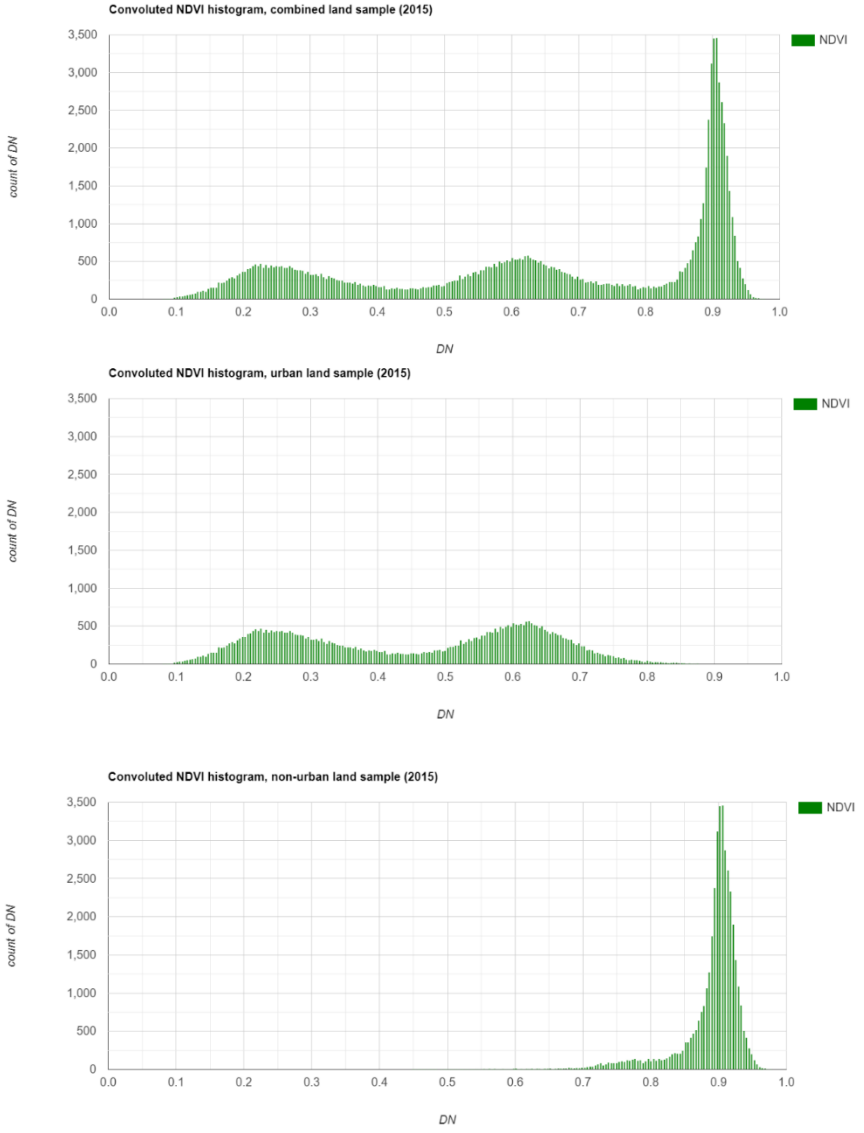

Figure 6 (3 vertical). Histograms of convoluted samples in combined and separated formats.

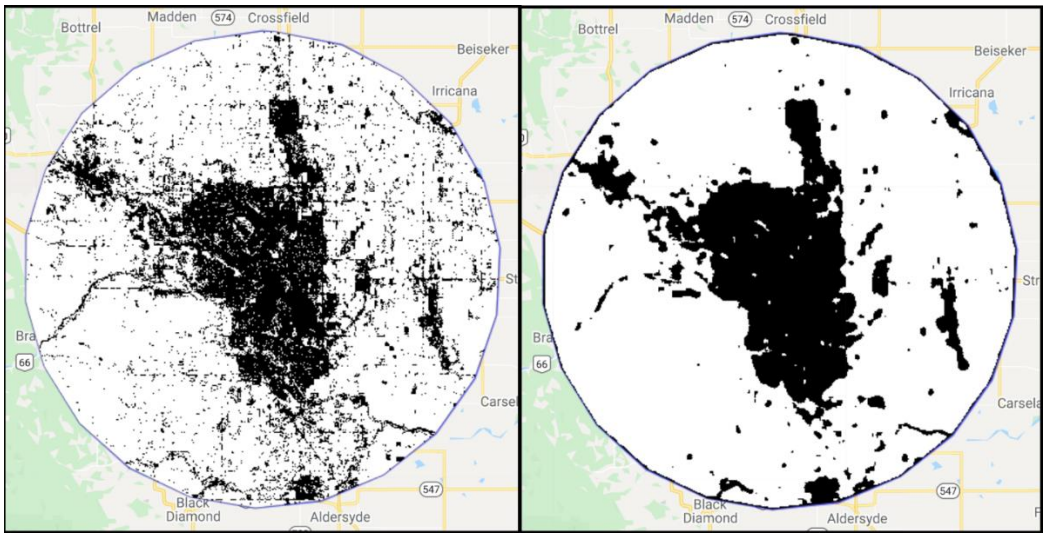

Figure 7. NDVIb band with a binary separation (0=black=urban, 1=white=non-urban). These images are the result of implementing the NDVI threshold of NDVIc = 0.7 on the base image (left) and with a 5x5 convolution filter (right) to remove high-frequency data and smooth out category cross-sampling.

NDBI band + Binary Threshold

Though each sample set was differentiated, it was decided that a low pass 5x5 convolution would help reduce the high frequency data that was crossing the differencing threshold. The ideal threshold looked to be around DN = -0.35 for the 2015 sample. The DN histograms of the convoluted sample sites showed a greater degree of DN value concentration with fewer tail values which resulted in less data overlap across the differencing threshold. In the set of convoluted NDBI histograms (*figures 10 & 11*), it appears that the differentiation threshold has moved closer to DN = -0.4. However, it was deemed prudent to keep the differencing threshold closer to the urban land samples peak value at DN = -0.35, because the NDBI is prone to overestimating built-up land. The NDBIc was then recoded along the differentiation threshold of DN= -0.35 into the urban/non-urban segmented NDBIb binary band (see *figure 9*).

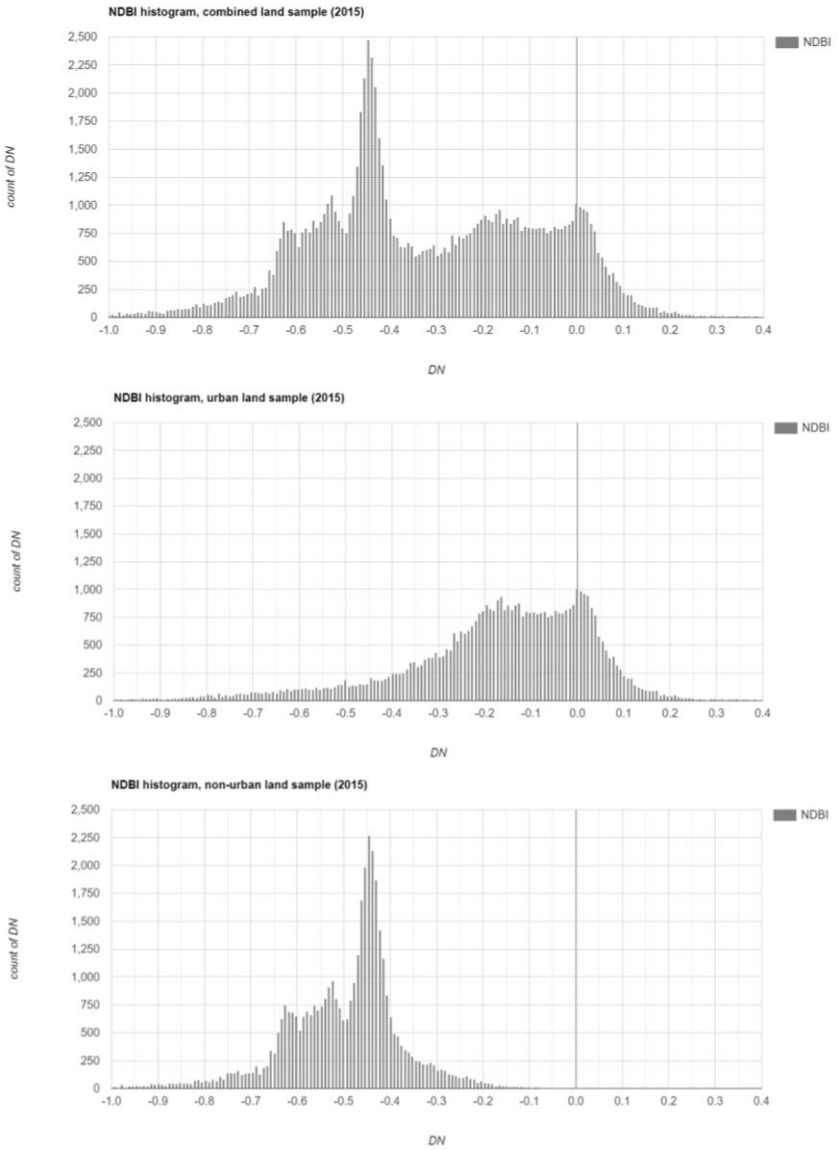

Figure 8 (3 vertical). NDBI histograms of unconvoluted samples in combined and separated formats.

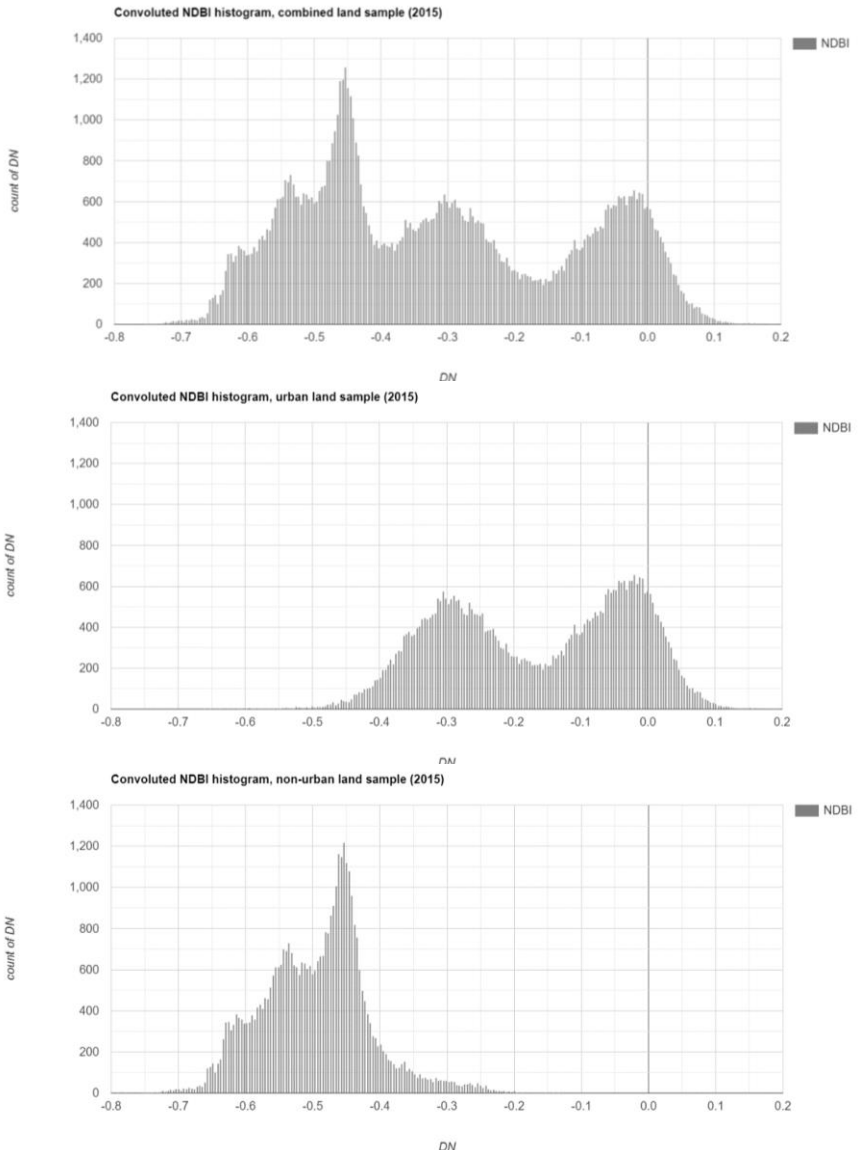

Figure 9 (3 vertical). NDBI histograms of convoluted samples in combined and separated formats.

Threshold Calibration. Initially it was thought that the two binary thresholds generated from the 2015 sample testing (above) could be applied to the other 7 images. However, the results were not satisfactory with the L5 and L7 datasets expressing urban and non-urban at different thresholds. This process of histogram analysis was performed for each image to ascertain a starting binary threshold which was then visually calibrated by the analyst to produce the best fidelity binary layer. The calibrated binary thresholds for each dataset are found in the *table 1*.

Table 1. Summary of NDVI and NDBI binary differentiation thresholds as determined by histogram analysis and manual calibration.

Dataset	$NDVI_b$ threshold	$NDBI_b$ threshold	Landsat
1995	0.55	-0.2	5
1990	0.55	-0.2	5
1995	0.6	-0.25	5
2000	0.6	-0.2	7
2005	0.6	-0.2	7
2010	0.6	-0.2	7
2015	0.7	-0.35	8
2020	0.7	-0.3	8

BUI band

The BUI band is created by subtracting the NDVI binary from the NDBI binary. Because these two datasets are identifying opposite features, the subtraction only mathematically acts on the discrepancies in land cover identification. Table X summarizes the land cover classification information as it is formatted in each respective dataset/image layer. These are listed in chronological order of data creation or transformations that lead to the BUI binary. This is reached not through more complex means of classification but through a semi-automatic segmentation built into the data transformation process.

Table 2. DN values for different land cover types after differencing and binary recoding. Based on 2015 sample, see table 2 for precise annual thresholds.

Land cover	Residential	Industrial	Woodland	Farmland	Waterbodies
NDVIc	< 0.7	< 0.7	> 0.7	> 0.7	< 0.7
NDBIc	> -0.35	> -0.35	< -0.35*	< -0.35*	< -0.35
NDVIb	0	0	1	1	0
NDBIb	1	1	0 or 1	0 or 1	0
BUIb	1	1	0 or -1	0 or -1	0
Classification	Urban		Non-urban		
* This data point is prone to overestimating urban land, however the inclusion of the more reliable NDVI in the BUI nullifies erroneously overclassified data					

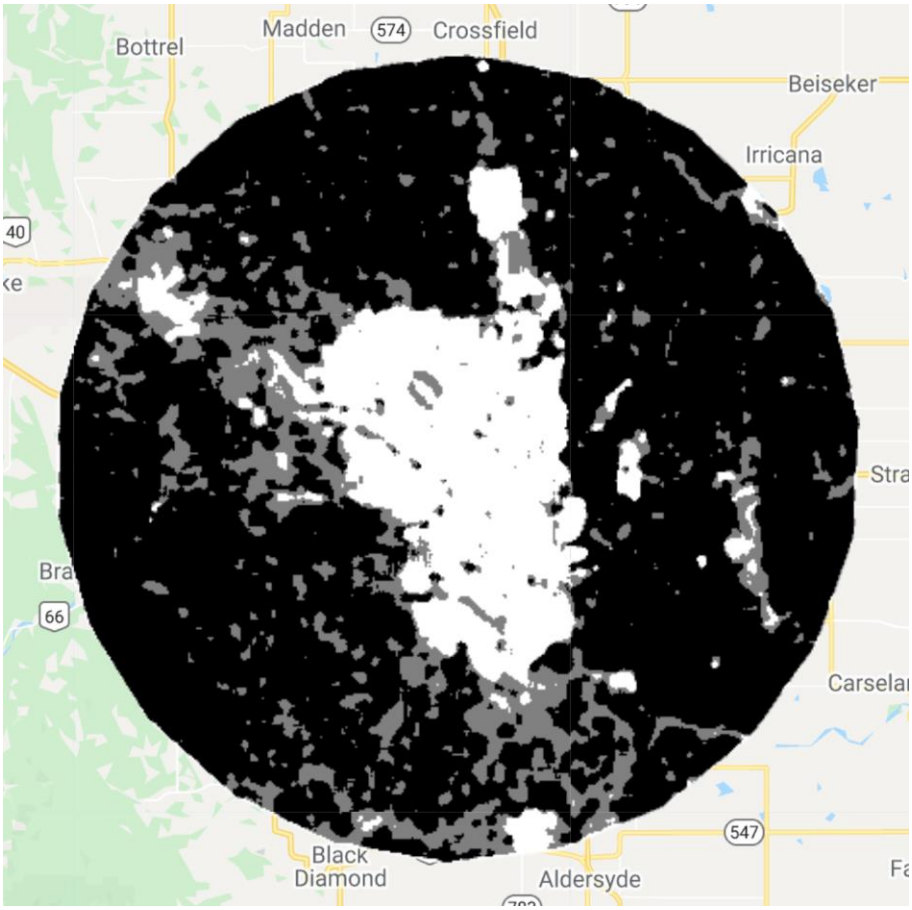

Figure 10. Binary BUI layer of Calgary study area. Urban areas are represented by the white polygons (DN=1) and black is non-urban (DN=-1). The grey polygons (DN=0) were declassified from the NDBI by the negating effect of the NDVI, these represent non-urban land cover as well.

ULE Data Vectorization and Editing

Using the parameters determined in the initial analysis phase, and urban land extent raster was generated for each 5-year time period between 1985 and 2020. This created 8 separate raster images that were put together as a time series dataset of ULE for Calgary and Edmonton. This image set was imported into ArcGIS Pro where they were vectorized.

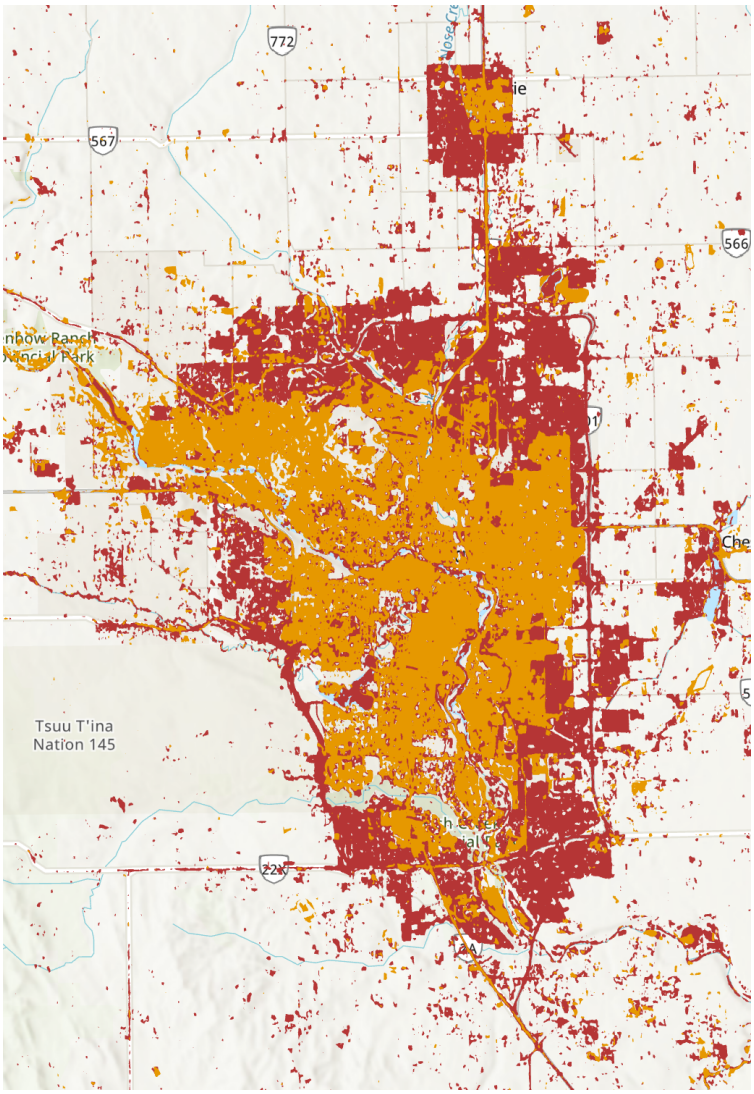

Figure 11. Vectorized City of Calgary UL extents from 1985 (orange) and 2020 (red) before noise deletion, manual editing, and aggregation.

Figure 13 demonstrates the need for cleaning and simplifying the UL extent polygons. Many small polygons beyond city limits are the result of small developments, barren land or industrial sites, none of which are of interest to this project. From the 2020 dataset, polygons of size less than or equal to 25 hectares were deleted and remaining polygons outside city limits were inspected with a satellite image underlay and deleted accordingly. Major holes in the urban polygons were manually filled with polygons and a merged Calgary region parklands dataset was deleted from the aggregated polygon file. This process resulted in a finished 2020 vector dataset.

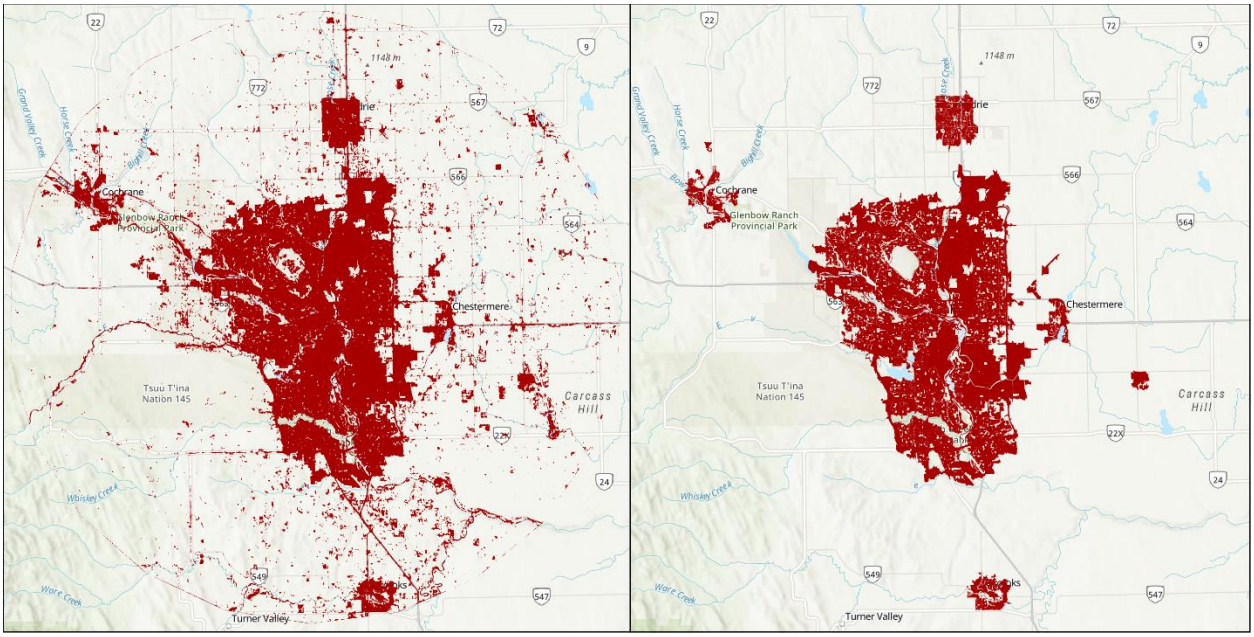

Figure 12. 2020 Calgary UL extent dataset before and after editing processes.

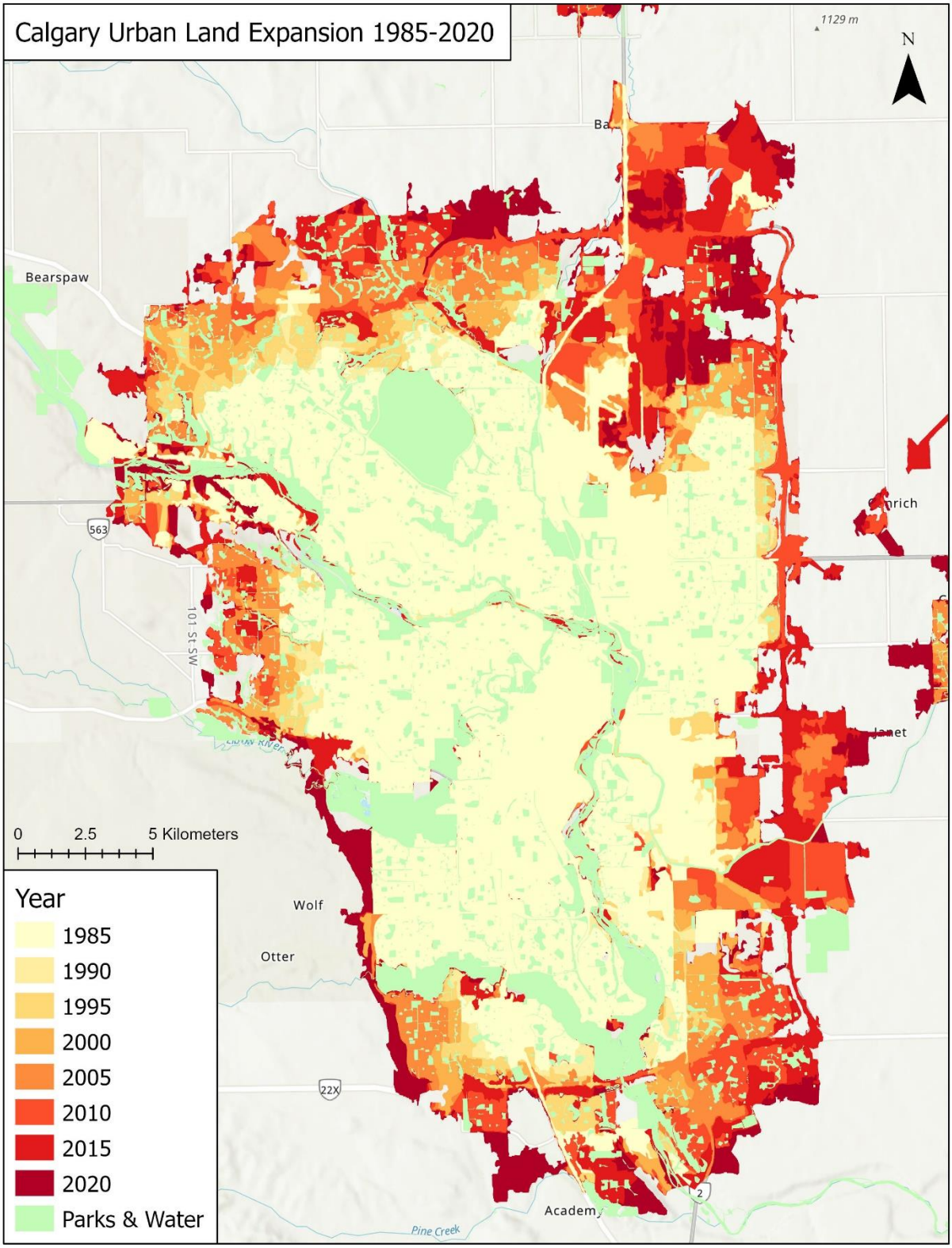

Figure 13. Urban Land Expansion of the City of Calgary between 1985 and 2020. Note significant spatial growth to the north and south with less gains on the east-west plane.

Radial Polyline Fan

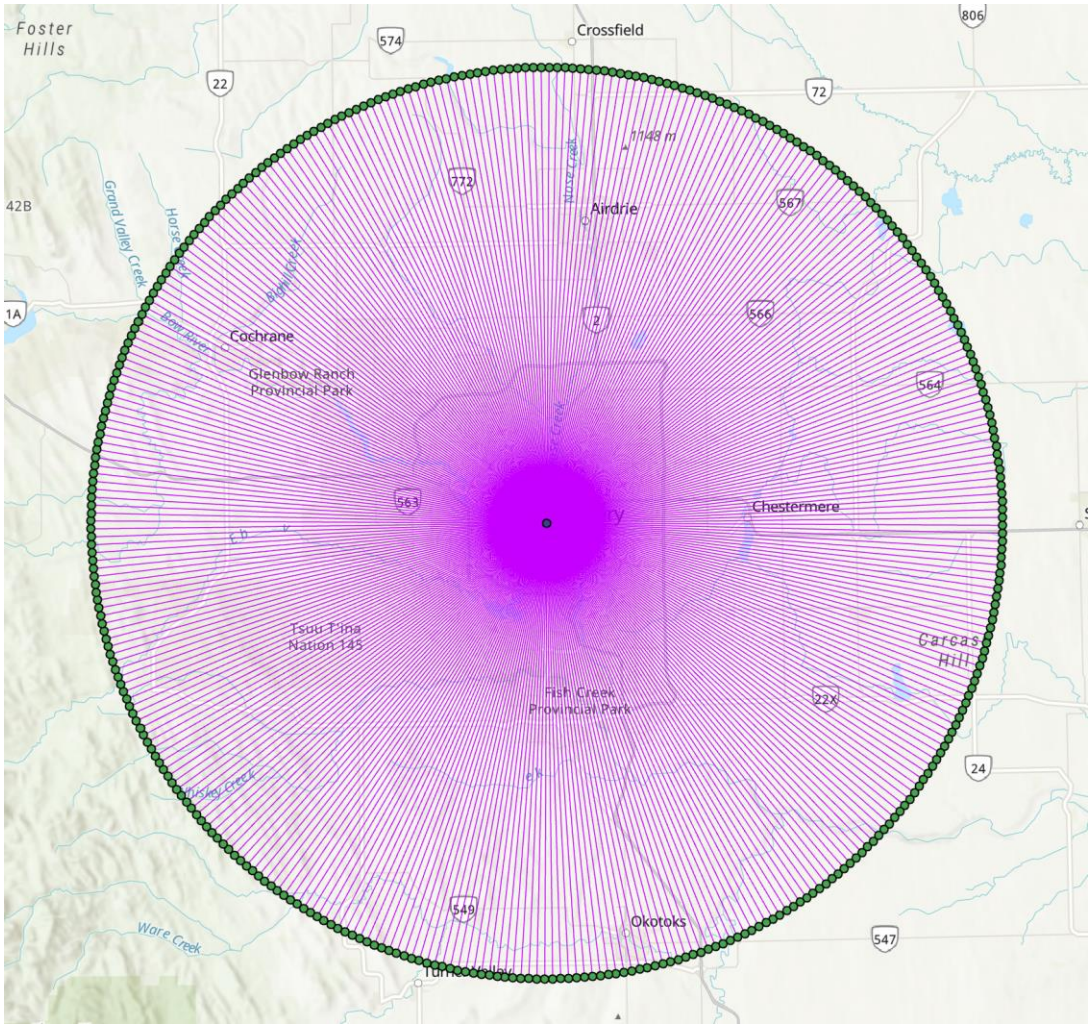

Figure 14. The 40-kilometer radial polyline fan used for measuring historical linear UL expansion.

The radial vector feature was constructed of 360 polylines at 1-degree intervals. The lines will be used to measure to urban land expansion along each given 1-degree plane where they intersect with the UL polygon datasets. 40-kilometer coverage made sure that adjacent communities were captured in the analysis. The external communities were Cochrane, Airdrie, Okotoks and Chestermere.

Time-Series

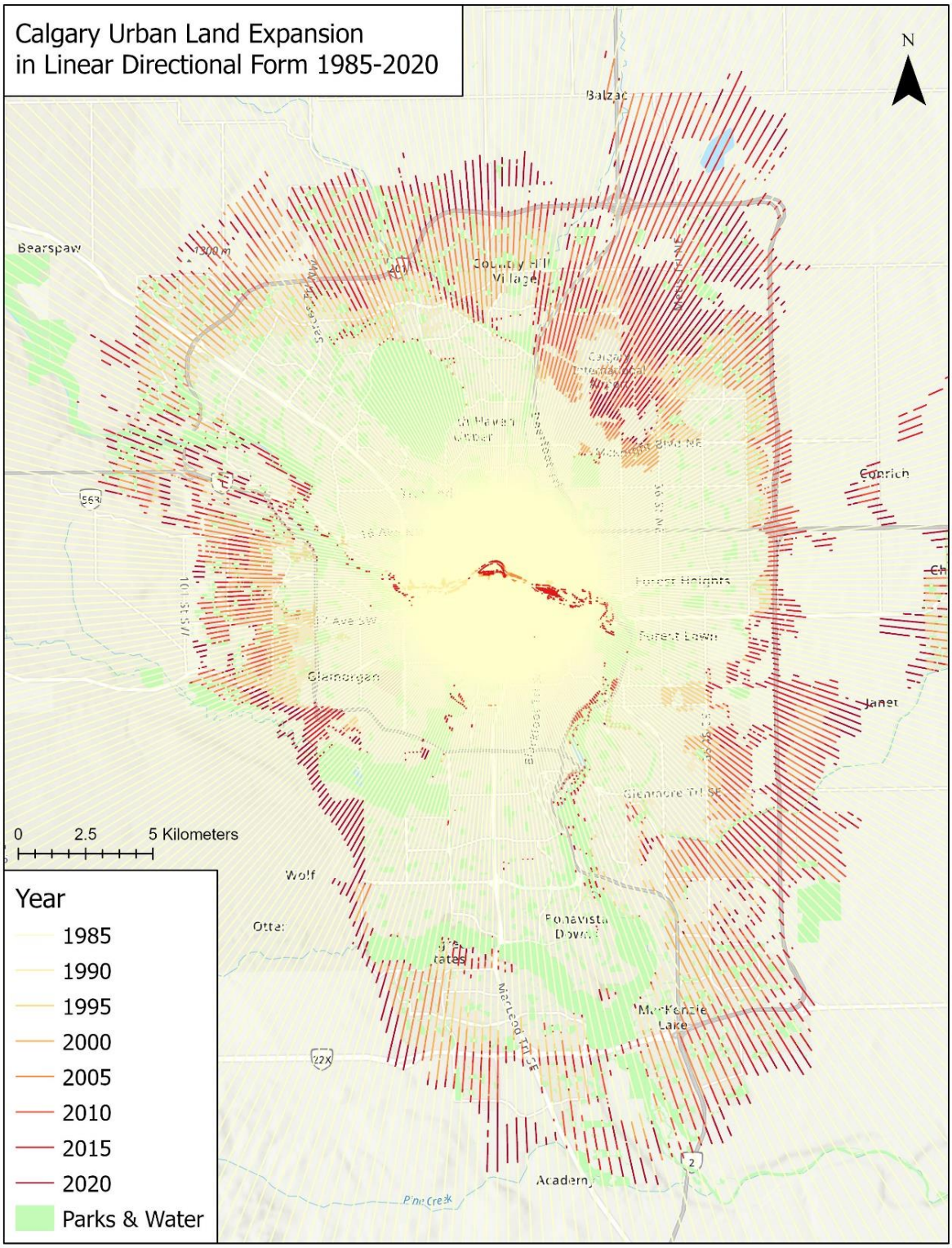

Figure 15. Calgary ULE map in linear directional data form.

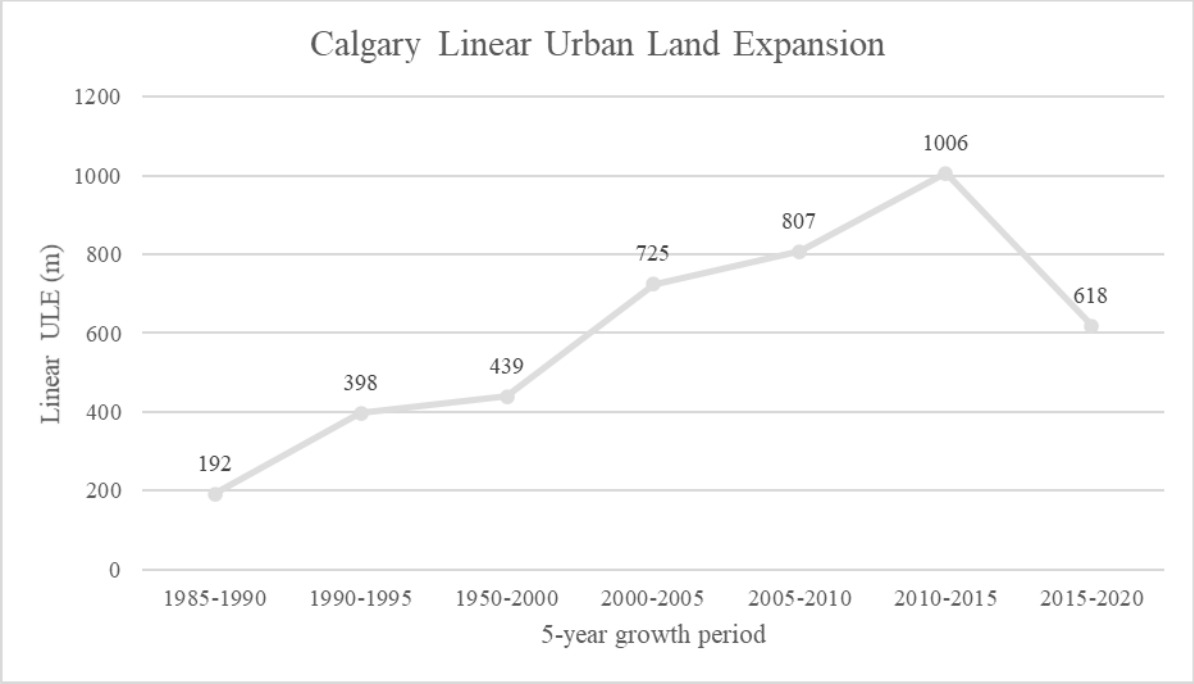

Figure 16. Average linear urban land expansion rate by 5-year increments, measured in meters.

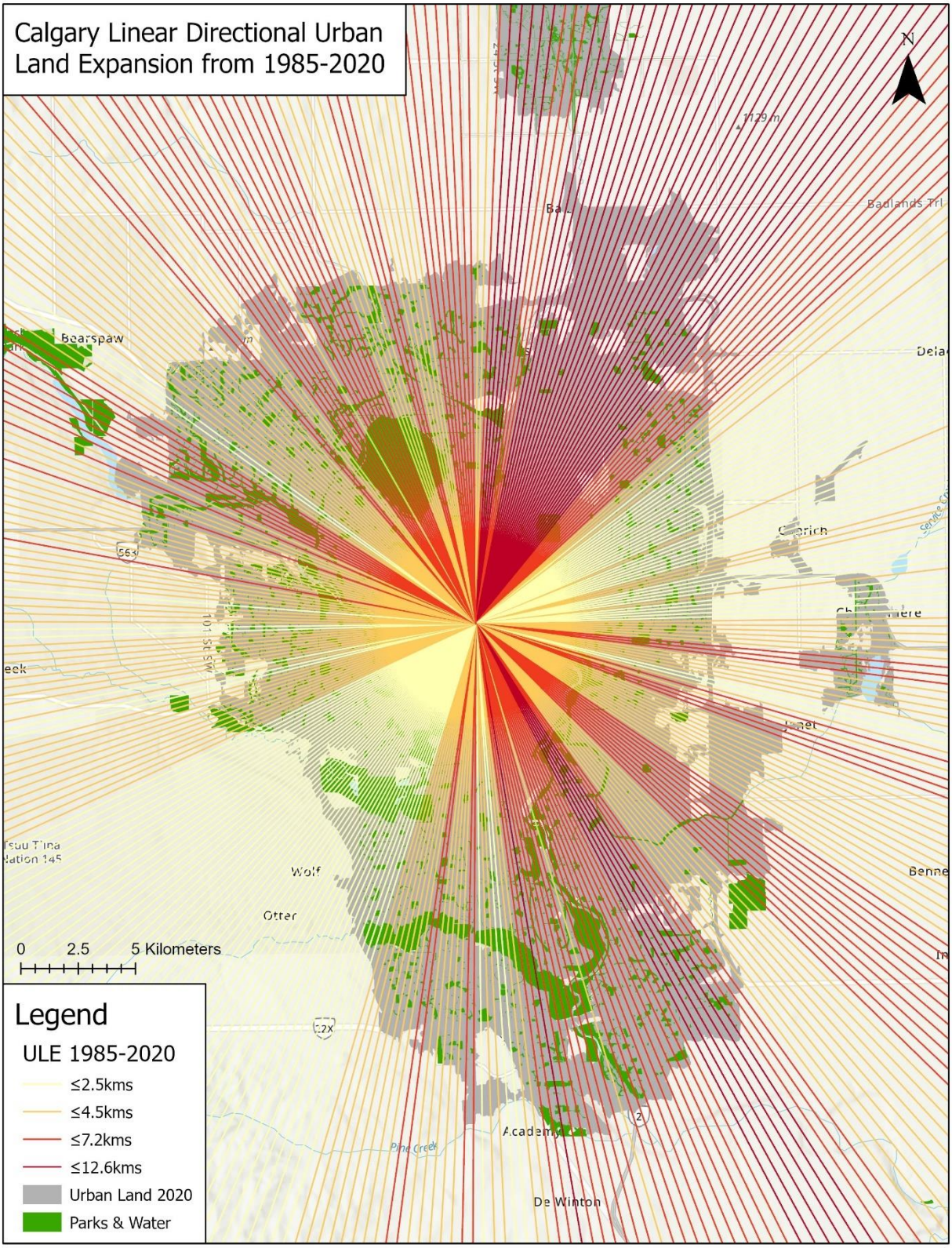

Figure 17. Map of linear directional ULE of Calgary between 1985 and 2020

Discussion

Modeling Accuracy

The method applied to perform the "semiautomatic" classification of urban lands was directly derived from Zha (2003). That paper was a case study assessing the efficacy of the built-up index (BUIb) method they proposed. Their 68 random pixel accuracy assessment revealed a 93% accuracy of the urban classified pixels. He et al (2010) later proposed an algorithmic change to the Zha method and tested the accuracy of both semiautomatic classification schemes. Their study claimed that the Zha method had a 64% accuracy, while their improved method had 86.3% accuracy. Because of the degree of manual verification and editing that was applied to each tail end dataset in the time series (1985 and 2020) and subsequently incorporated into the interim datasets through data transformations, it would not have been meaningful to perform an accuracy assessment on the unedited BUIb or edited UL extents. Furthermore, it is not within the scope of this project to assess the strength of the 'semiautomatic' urban land classification method because it was only intended to be used as a preliminary data creation method. However, it is worth noting that in this case the BUI binary method was almost certainly below the 92.3% accuracy assessment of the method authors and was likely no lower than the 64% accuracy claimed by He et al (2010). Had the observable accuracy been near 92.3%, the dataset would not have needed such extensive manual editing work.

Modeling Method

The modeling method presented significant errors of both omission and commission, which ultimately created the need for extensive manual editing to be implemented to both reign-in and fill-in the datasets by overlaying them on the RGB Landsat images. As a derivative of the

extensive manual vector editing, merging and clipping functions needed to be implemented up and down the time-series to integrate the changes on the 1985 and 2020 into the rest of the time-series datasets. This significantly increased to workload considering the method was termed "semiautomatic". Other more cutting-edge methods could be applied in a future iteration of this study. Within Google Earth Engine it is possible to apply machine learning (ML) using training samples to perform land cover classifications. Tensorflow ML is integrated with GEE. This method would have likely been more accurate and possibly more expedient. Additionally, as of 2019 Google's AI platform can be plugged into GEE via Colab (Rao, 2019). AI-based image recognition would likely exceed the accuracy of any more rudimentary spectra-based models such as the one applied. However, once again comparative analysis of land-cover classification methodologies was beyond the scope of this project.

Data Model Assumptions

The methodology applied to create the time-series ULE dataset was intendent to cut down on the amount of manual digitization by implementing a semi-automatic classification approach. In this respect it was somewhat successful. Throughout the construction of the UL extent datasets, two assumption were made which precipitated two logical operations to be implemented. The major assumptions were the (1) constancy and (2) permanence of urban development: that throughout the study period the city was always growing, and never de-developing. The only observed instances of de-development was the natural reclamation of the gravel pit in Nose Hill Park and errors of omission. However, the first object was not consequential because it was clipped out by the park and waterbodies exclusion.

This logical operation of the constancy assumption is that going backwards chronologically, more recent datasets could be used to delimit previous extents. This operation would cut down on errors of commission. This logic dictates that a given plot that is undeveloped in 2020 would have also been undeveloped in all previous 5-year periods. According to this assumption of development constancy, each dataset was clipped down using the extent of the 5-year newer ULE extent.

Secondly, moving up through datasets chronologically, it is reasoned that due to the permanence of urbanization, any given piece of lands developed in 1985 would remain developed in all future 5-year increments of data. This logic justified merging earlier UL polygons into newer datasets to ensure there were no cases of omission error where land was only developed in an earlier dataset. It is reasonable to expect no degrowth in Calgary because the city has consistently grown in population and spatial footprint throughout the study periods. Imperfections in the semiautomatic classification and manual editing resulted in instances of omission errors that would have represented de-development of urban properties. The addition of the merging process resolved this logical inconsistency.

Land Developability

Not all land is physically developable. Examples of this include water bodies, riparian areas and steep or unstable slopes. Additionally, lands can become protected from development because of land governance, politics or environmental sensitivity. Examples of this include indigenous reserves, parks and greenbelts. This model could have been structured with greater detail to establish such exclusions; however, the simple classification approach is still effective

because the redistributive effect of undevelopability on city growth is captured in the linear urban growth pace measurements.

Though waterbodies and parks are excluded from direct measurement in the linear urban growth pace, their broader influence on the pace of development is captured. Parks are a necessary feature of great cities and communities, which is why planners spatially distribute parks to ensure accessibility for all citizens. This relatively even distribution means that the uncounted (in the linear model) effect of parks development on linear urban growth is somewhat evened out across each directional measurement. Parks also have a market-based displacement effect on developable land supply. In the simplest terms, where a park fails to meet a market-demand for housing at the park site, the demand is met by a housing purchase or land development elsewhere, which in turn influences the outward growth of the city. For this reason, the influence of land protection within the developed portion of cities is accounted for as a necessary aspect of city building.

Additionally, small greenspaces that are not designated as parks were convoluted into the urban land cover category because of low-pass filtering. Assuming the land development paradigm does not change substantially, the effect of land development exclusions on the pace of development should remain similar going forward to the effect that was captured within this methodology. Land that was physically undevelopable for geophysical reason is typically incorporated into the managed parks system. This is exemplified by the extensive parks system in Calgary that is made up of many bluffs and steep hills that were presumably deemed undevelopable by land development engineers.

Pace and Geometry of ULE

Surprisingly, the average periodized linear ULE shows a clear increasing trend between 1985 and 2015 (*figure 18*). Though acceleration of areal/surficial ULE is almost a given considering the critical mass-like nature of city growth, the result of which is somewhat of an exponential areal growth curve under the current development paradigm. There should be somewhat of an asymmetric relationship between linear and areal ULE. Basic geometry dictates that as cities become bigger, a greater the amount of land surface that needs to be urbanized to linearly extend the city by a fixed distance. This relationship could even result in a decelerating linear growth rate while the areal growth rate is accelerating. This odd case could occur in very large cities, where the addition of only a small amount of linear urbanized distance can result in massive population and urbanize land growth.

Adjacent communities were included in this study because of their effect on regional growth. The growth of communities like Cochrane, Okotoks, Chestermere and Airdrie are inextricably tied to the growth, development and economic strength of Calgary. Their close regional ties mean that these communities collectively are worth consideration as a single regional urban entity. It is important to consider that these communities add two extra growth-frontiers to each polyline that passed through them. For example, a polyline that aligned with Okotoks would have the growth frontier on the southern perimeter of the central city (Calgary), as well as an additional growth-frontier on either side of Okotoks. Though this has somewhat of a distortive effect on the data model, it was deemed important to include them anyway. Unsurprisingly, the distortions were not hugely consequential. Because of the size of those communities, they grow at a much slower lineal pace.

The planes with fastest total lineal growth during the 35-year study period were the south-east and north-east cardinal directions. The southeast development was driven largely by residential development and the expansion of the Stoney Trail ring road. The northeast directional growth plane had the highest growth of any LDULE measurements. This was due to a convergence of growth factors. A large increase in industrial lands around the airport, residential neighbourhoods east of the airport with commensurate retail development, the construction of the Stoney Train ring road north quadrant, residential growth in Airdrie (which intersected with several polylines) and the development of lands outside of the ring road (industrial lands near CrossIron Mills and Balzac power station).

Rate of Change

Interestingly, Calgary's rate of linear ULE of 618m from 2015-2020 represented a quite drastic drop of around 40% from the 2010-2015 rate of 1006m. Seeing as Calgary is a corporate center for the oil and gas industry in western Canada, the 2014 drop in oil prices maybe have been a factor in this drop in the ULE rate. The economic climate in the city changed drastically because of this economic event and growth driven housing expansion may have slowed down as a result. Another possible factor at play is that the 2010-2015 measurement was anomalously high because a large amount of land was broken for the construction of the Stoney Trail in the south and east quadrants of the city and large tracts of industrial lands were developed near the airport (*see figure 15 map,* 2015 expansion tranche).

Transportation infrastructure and industrial land development can urbanize large amounts of land very quickly compared to residential development. The sudden drop in industrial development caused by the 2014 oil bust may have been even more drastic than a slowdown in

residential development led ULE. The development of Stoney Trail alone could have added several dozen meters to the average linear ULE because of the sheer volume off land required to build the transportation and utility corridor. However, the 2010-2015 measurement is not necessarily anomalous because it was keeping with the trend up to that point. It is possible that given the current size of Calgary, a linear expansion pace of 1km per 5 years is not sustainable without a symmetric expansion of housing, industrial and public infrastructural lands. These symmetrical conditions can only exist when the regional economy is experiencing a sustained period of growth, which is fairly rare.

Density & Deceleration

Some recent outer rim neighbourhoods will have a higher density pattern when compared to the development paradigm of 1950s-2000s where entire developments were land-inefficient single-detached homes. These new outer rim neighbourhoods will probably be more like what suburban development will resemble going forward with mixed-use and mixed density that is characteristic of edge city thought in urban planning circles. Though this process of increasing density through new forms of urban development will be an incremental long-term project, some examples of higher-density development paradigms are emerging.

Edmonton has successfully built the Windermere neighbourhood outside of the Anthony Henday ring road, with a commercial district, condo towers and a mixed density of housing options. St. Albert has successfully developed several apartment towers throughout the city with incorporated commercial ground floors in a community that is known for being a family-oriented suburb made almost entirely of single-detached homes.

Though the economic explanation for Calgary's recent LULE slowdown may be more compelling, it is possible that edge city style development and incrementally higher density suburbs being developed since 2015 are responsible for some of the drop in linear ULE. On aggregate, more land-efficient development could decrease both linear and areal ULE rates barring a surge in housing or commercial space demand that is more powerful than the deflationary effect of rising density on ULE metrics. Moving forward it would be interesting to see if the 30-year trend of rising linear ULE rate returns.

Applications & Further Research

Time-to-Development Prediction Models. While most ULE forecasts are made by multiplying population growth forecasts by present development density, perhaps a prediction method could emerge that utilises linear directional ULE as a prediction variable. This project demonstrated the possibility of analysing the change of centroid-to-fringe polylines over various time periods in terms of the pace of development or trend in terms of linear distance growth in specific outward directions. This directional data could be consequential for the prediction of time-to-development for specific developable properties beyond city limits. This differs from the typical research perspective of concern for agricultural land loss, which results in area/surface focused research, modelling, and prediction. Even less discussed is the utility of plot specific time-to-development ULE predictors for conservationists to focus their efforts sequentially, as opposed to organizing their efforts according to complex environmental sensitivity studies or subjective levels of environmental concern. Such a model could increase the efficiency and efficacy of conservationists by helping them determine which lands are closest to being lost to urbanization.

LULE, AULE & Density. A comparative study of Linear ULE (LULE), Areal ULE (AULE) and development density would likely result in interesting insights about the relationship between city expansion and land loss. Analytic tools could be developed for city planning departments that target expansion rates and the density of development approvals. Hypothetically, urban development could be regulated to ensure a decelerating rate LULE. Though linear city growth is an abstracted metric from true land conservation, which is better measured by AULE, it could be used as a goal post to determine reasonable and achievable improvements in long-term land conservation. Additionally, LULE captures the impact of dispersal on urban mobility better than AULE does. From a transportation planning perspective, indexing city growth to reduce the rate of LULE could reduce the need for new automobile-oriented transportation infrastructure and indirectly make public transportation more viable by increasing population density and reducing distances travelled. Something like this could hypothetically be an alternative to greenbelting or other forms of land development restrictions.

Weighted Averaging LULE. A proximity based weighted averaging system would have improved the insights of the model presented in *figure 19*. The directional data was relatively well distributed, with mostly consistent clustering of rates along adjacent lines. For that reason, this instance did not demonstrate a pressing need for data smoothing. However, some softening of the data may have provided a more aggregated and holistic perspective of which sectors of the city were growing at the fastest rates. This could have been implemented by averaging the ULE rate of each polyline with the weighted values of a few adjoining lines. Further research of this topic should implement some proximity-weighted averaging to remove any potential noise in the final data.

Conclusion

Globally, urbanisation appears to be an unstoppable force as the populations of cities swell and the socio-economic transformations of the information age enshrine urban regions as the main economic drivers of the global economy. Within this context, urbanisation presents a unique set of opportunities and challenges. Well planned and densified cities can render essential services efficiently and provide people with myriad opportunities to improve their lives. On the other hand, unfettered urbanisation threatens to destabilize the fragile relationship between humankind and nature. Cities that urbanise poorly can become environmental, human health and socio-political disaster zones. We must begin to accelerate efforts to build cities upward, not outwards, in order to accommodate growing urban populations in a more sustainable way and not harm the important natural mechanisms that render essential ecosystem services to humanity. For this reason, it is important to monitor the growth of urban regions throughout the world.

This paper proposed a methodology to assess the rate at which cities are expanding linearly. This Linear Urban Land Expansion (LULE) measurement was applied to Calgary, Alberta, a city on the western Canadian prairies that has experienced explosive growth over the last four decades. The method used Landsat imagery to determine the evolution of the urbanized footprint of the city between 1985 and 2020. Google Earth Engine (GEE) was used to analyse the satellite imagery archive efficiently using powerful cloud infrastructure. Though the project was not completed entirely in GEE, it is conceivable that all the functions necessary to create these metrics could be moved into GEE, making the project highly reproducible across any urban region throughout the world. The results showed a nuanced build-out of the city with higher rates of linear expansion in certain quadrants. A relatively stable accelerating trend was also observed between 1985-2015, before a significant drop between 2015 and 2020.

Bibliography

Ali, A. K. (2008). Greenbelts to Contain Urban Growth in Ontario, Canada: Promises and Prospects. *Planning, Practice & Research*.

Angel, S., Parent, J., Civco, D. L., & Blei, A. M. (2010). *The Persistent Decline in Urban Densities: Global and Historical Evidence of Sprawl.* Lincoln Institute of Land Policy.

Angel, S., Parent, J., Civco, D., Blei, A., & Potere, D. (2011). The dimensions of global urban expansion: Estimates and projections for all countries, 2000–2050. *Progress in Planning*.

Bren d'Amour, C., & al, e. (2016). Future urban land expansion and implications for global croplands. *Proceedings of the National Academy of Sciences of the United States of America*.

Canadian Mortage and Housing Corporation. (2019). *Government of Canada offers Homeownership Incentives*. Retrieved from Finance and Investing: https://www.cmhc-schl.gc.ca/en/finance-and-investing/mortgage-loan-insurance/the-resource/government-of-canada-offers-homeownership-incentives

Caron Malenfant, E., Milan, A., Charron, M., & Belanger, A. (2007). *Demographic Changes in Canada from 1971 to 2001 Across and Urban-to-Rural Gradient.* Ottawa: Statistics Canada.

City of Airdrie. (2018). *Airdrie Greenspace*. Retrieved from City of Airdrie Open Data: https://data-airdrie.opendata.arcgis.com/datasets/airdrie-greenspace?geometry=-114.099%2C51.267%2C-113.896%2C51.304

City of Calgary. (2020). *Parks Sites*. Retrieved from City of Calgary Open Data: https://data.calgary.ca/Recreation-and-Culture/Parks-Sites/i9fu-gjqj

City of Chestermere. (2020). *Parks - Open*. Retrieved from Chestermere Open Data: https://data-chestermere.opendata.arcgis.com/datasets/parks-open?geometry=-114.106%2C51.002%2C-113.539%2C51.078&showData=true

City of Edmonton. (2017). *Annual Growth Montoring Report 2017.* Edmonton: City of Edmonton.

City of Edmonton. (2019). *Hydrology*. Retrieved from City of Calgary Open Data: https://data.calgary.ca/Environment/Hydrology/a2cn-dxht

Clarke, K. C. (2000). *Home*. Retrieved from Project Gigalopolis: http://www.ncgia.ucsb.edu/projects/gig/About/bkOverview.html

Davies, W. K., & Baxter, T. (1997). Commercial Intensification: the Transformation of a Highway-orientated Ribbon. *Geoforum*.

DesRoches, R., Comerio, M., Eberhard, M., Mooney, W., & Rix, G. J. (2011). *Overview of the 2010 Haiti Earthquake.* Earthquake Spectra.

Dodman, D., Leck, H., Rusca, M., & Colenbrander, S. (2017). African Urbanisation and Urbanism: Implications for risk accumulation and reduction. *International Journal of Disaster Risk Reduction*.

Eigenbrod, F., Bell, V. A., Davies, H. N., Heinemeier, A., Armsworth, P. R., & Gaston, K. J. (2011). The impact of projected increases in urbanization on ecosystem services. *Proceedings of the Royal Society B*.

Filion, P., & Bunting, T. (2015). Urban Transitions: The History and Future of Canadian Urban Development. In P. Filion, M. Moos, T. Vinodrai, & R. Walker, *Canadian cities in transition: perspectives for an urban age* (pp. 17-37). Don Millis, Ontario: Oxford.

Gao, J., Wei, Y. D., Chen, W., & Chen, J. (2014). Economic transition and urban land expansion in Provincial China. *Habitat International*.

Global Change Data Lab - Oxford University. (2018). *Urbanization over the past 500 years, 1500 to 2016*. Retrieved from Our World in Data: https://ourworldindata.org/grapher/urbanization-last-500-years

Goodman, C. B. (2019). The Fiscal Impacts of Urban Sprawl: Evidence From U.S. County Areas. *Public Budgeting and Finance*.

Google Earth. (2019, Sept). *Down to Earth with AI Platform*. Retrieved from Google Earth and Earth Engine - Medium blog: https://medium.com/google-earth/down-to-earth-with-ai-platform-7bc363abf4fa

Government of Alberta. (2017). *Parks and Protected Areas in Alberta*. Retrieved from Alberta Open Government Program: https://open.alberta.ca/opendata/gda-6b96341f-2e19-4885-98af-66d12ed4f8dd

Güneralp, B., & al, e. (2019). Trends in urban land expansion, density, and land transitions from 1970 to 2010: a global synthesis. *Environmental Research Letters*.

Hansen, M. C., Potapov, P. V., Moore, R., Hancher, M., & Turubanova, S. (2013). High-Resolution Global Maps of 21st-Century Forest Cover Change. *Science*.

Hathout, S. (2002). The use of GIS for monitoring and predicting urban growth in East and West St Paul, Winnipeg, Manitoba, Canada. *Journal of Environmental Management*.

He, C., Shi, P., Xie, D., & Zhao, Y. (2010). Improving the normalized difference built-up index to map urban built-up areas using a semiautomatic segmentation approach. *Remote Sensing Letters*.

L3Harris Geospatial. (2013, Aug). *Digital Number, Radiance, and Reflectance*. Retrieved from Blog: https://www.l3harrisgeospatial.com/Learn/Blogs/Blog-Details/ArtMID/10198/ArticleID/16278/Digital-Number-Radiance-and-Reflectance

Liu, X., Hu, G., Chen, Y., Li, X., Xu, X., Li, S., . . . Wang, S. (2018). High-resolution multi-temporal mapping of global urban land using Landsat. *Remote Sensing of the Environment*.

Malik, A., & Abdalla, R. (2017). Agent-based modeling for urban sprawl in the region of Waterloo, Ontario, Canada. *Modelling Earth Systems and Environment*.

McCarthy, M. P. (1986). The Politics of Suburban Growth: A Comparative Approach. In G. A. Stelter, & A. F. Artibise, *Power and Place* (pp. 323-339). Vancouver: University of British Columbia Press.

Meier, P. (2012). How Crisis Mapping Saved Lives in Haiti. *National Geographic*.

Millward, H. (2008). Evolution of Population Densities: Five Canadian. *Urban Geography*.

NASA. (2020). *Landsat 6*. Retrieved from Landsat Science: landsat.gsfc.nasa.gov/landsat-6/

Natural Capital Project, Stanford Univeristy. (n.d.). *InVEST*. Retrieved from Natural Capital Project: https://naturalcapitalproject.stanford.edu/software/invest

Pramanik, M., & Stathakis, D. (2015). Forecasting urban sprawl in Dhaka city of Bangladesh. *Environment and Planning B: Planning and Design*.

Rao, K. (2019). *New Earth Engine Features announced at Geo for Good Summit 2019*. Retrieved from towards data science - Medium Blog: https://towardsdatascience.com/new-earth-engine-features-announced-at-geoforgood-summit-2019-57c33ef48bb8

Ritchie, H. (2018). *Urbanization*. Retrieved from Our World in Data: https://ourworldindata.org/urbanization

Simone, D., & Walks, A. (2019). Immigration, race, mortgage lending, and the geography of debt in Canada's global cities. *Geoforum*.

Statistics Canada. (2002). *A profile of the canadian population: where we live.* Retrieved from http://geodepot.statcan.ca/diss/highlights/text_e.pdf

Statistics Canada. (2005). *The Loss of Dependable Agricultural Land in Canada.* Ottawa: Statistics Canada.

Statistics Canada. (2018, May). *Canada Goes Urban.* Retrieved from Statistics Canada: https://www150.statcan.gc.ca/n1/pub/11-630-x/11-630-x2015004-eng.htm

Statistics Canada. (2019, March). *Canada's population estimates: Subprovincial areas, July 1, 2018.* Retrieved from Statistics Canada: https://www150.statcan.gc.ca/n1/daily-quotidien/190328/dq190328b-eng.htm

Sun, H., Forsythe, W., & Waters, N. (2007). Modeling Urban Land Use Change and Urban Sprawl: Calgary, Alberta, Canada. *Networks and Spatial Economics*.

Tan, M., Li, X., Xie, H., & Lu, C. (2005). Urban land expansion and arable land loss in China—a case study. *Land Use Policy*.

The World Bank. (2018). *Population growth (annual %)*. Retrieved from The World Bank - Data: https://data.worldbank.org/indicator/SP.POP.GROW

Town of Cochrane. (2020). *Cochrane Open Spaces*. Retrieved from Town of Cochrane Open Data: https://data-cochranegis.opendata.arcgis.com/datasets/cochrane-open-spaces?geometry=-114.676%2C51.149%2C-114.268%2C51.224

Town of Okotoks. (2020). *Parkspace*. Retrieved from Okotoks Open Data Portal: https://data-okotoks.opendata.arcgis.com/datasets/e0551b6867044fbeb05381ac9758c5c9_20

UN Department of Economic and Social Services. (2019). *World Population Prospects 2019*. Retrieved from Population Dynamics Data Center: https://population.un.org/wpp/Graphs/DemographicProfiles/Line/156

United Nations - DESA. (2009). *Urban and Rural Areas 2019.* Retrieved from United Nation Department of Economic and Social Affairs, Population Division: https://www.un.org/en/development/desa/population/publications/pdf/urbanization/urbanization-wallchart2009.pdf

United States Geological Survey. (2018). *Landsat Collection 1*. Retrieved from Landsat Collections: https://www.usgs.gov/core-science-systems/nli/landsat/landsat-collection-1?qt-science_support_page_related_con=1#qt-science_support_page_related_con

Vaz, E., Buckland, A., & Worthington, K. (2013). A regional spatial-retrofitting approach (rsra) to geovisualise regional urban growth: an application to the golden horseshoe in canada. *Journal of Spatial and Organizational Dynamics*.

Vernburg, P. H., van de Steeg, J., Veldkamp, A., & Willemen, L. (2009). From land cover change to land function dynamics: A major challenge to improve land characterization. *Journal of Environmental Management*.

Wihbey, J. (2017). Boundary Issues: The 2016 Atlas of Urban Expansion Indicates Global Dedensification. *Cityscape: A Journal of Policy Development and Research*.

Zha, Y., Gao, J., & Ni, S. (2003). Use of normalized difference built-up index in automatically mapping urban areas from TM imagery. *International Journal of Remote Sensing*.

Zhang, D., Huang, Q., He, C., & Wu, J. (2017). Impacts of urban expansion on ecosystem services in the Beijing-Tianjin- Hebei urban agglomeration, China: A scenario analysis based on the Shared Socioeconomic Pathways. *Resources, Conservation & Recycling*.